

## Article

# Integrating Remote Sensing Techniques and Meteorological Data to Assess the Ideal Irrigation System Performance Scenarios for Improving Crop Productivity

Heman Abdulkhaleq A. Gaznayee <sup>1,\*</sup>, Sara H. Zaki <sup>1</sup>, Ayad M. Fadhil Al-Quraishi <sup>2,\*</sup>, Payman Hussein Alihsan <sup>1</sup>, Kawa K. Hakzi <sup>3,\*</sup>, Hawar Abdulrzaq S. Razvanchy <sup>3</sup>, Michel Riksen <sup>4</sup> and Karrar Mahdi <sup>4</sup>

<sup>1</sup> Department of Forestry, College of Agricultural Engineering Science, Salahaddin University-Erbil, Erbil 44003, Iraq; sarah.haiman90@gmail.com (S.H.Z.); payman.alihsan@su.edu.krd (P.H.A.)

<sup>2</sup> Petroleum and Mining Engineering Department, Faculty of Engineering, Tishk International University, Erbil 44001, Iraq

<sup>3</sup> Department of Soil and Water, College of Agricultural Engineering Science, Salahaddin University-Erbil, Erbil 44003, Iraq; hawar.sadiq@su.edu.krd

<sup>4</sup> Soil Physics and Land Management Group, Wageningen University & Research, 6700 AA Wageningen, The Netherlands; michel.riksen@wur.nl (M.R.)

\* Correspondence: heman.ahmed@su.edu.krd (H.A.A.G.); ayad.alquraishi@tiu.edu.iq (A.M.F.A.-Q.); kawahakzy@gmail.com (K.K.H.)

**Abstract:** To increase agricultural productivity and ensure food security, it is important to understand the reasons for variations in irrigation over time. However, researchers often avoid investigating water productivity due to data availability challenges. This study aimed to assess the performance of the irrigation system for winter wheat crops using a high-resolution satellite, Sentinel 2 A/B, combined with meteorological data and Google Earth Engine (GEE)-based remote sensing techniques. The study area is located north of Erbil city in the Kurdistan region of Iraq (KRI) and consists of 143 farmer-owned center pivots. This study also aimed to analyze the spatiotemporal variation of key variables (Normalized Difference Moisture Index (NDMI), Normalized Difference Vegetation Index (NDVI), Precipitation (mm), Evapotranspiration (ET<sub>o</sub>), Crop evapotranspiration (ET<sub>c</sub>), and Irrigation (Hours), during the wheat-growing winter season in the drought year 2021 to understand the reasons for the variance in field performance. The finding revealed that water usage fluctuated significantly across the seasons, while yield gradually increased from the 2021 winter season. In addition, the study revealed a notable correlation between soil moisture based on the (NDMI) and vegetation cover based on the (NDVI), and the increase in yield productivity and reduction in the yield gap, specifically during the middle of the growing season (March and April). Integrating remote sensing with meteorological data in supplementary irrigation systems can improve agriculture and water resource management by boosting yields, improving crop quality, decreasing water consumption, and minimizing environmental impacts. This innovative technique can potentially enhance food security and promote environmental sustainability.

**Keywords:** irrigation system; NDVI; NDMI; meteorological data; center pivot



**Citation:** Gaznayee, H.A.A.; Zaki, S.H.; Al-Quraishi, A.M.F.; Alihsan, P.H.; Hakzi, K.K.; Razvanchy, H.A.S.; Riksen, M.; Mahdi, K. Integrating Remote Sensing Techniques and Meteorological Data to Assess the Ideal Irrigation System Performance Scenarios for Improving Crop Productivity. *Water* **2023**, *15*, 1605. <https://doi.org/10.3390/w15081605>

Academic Editor: Guido D'Urso

Received: 16 March 2023

Revised: 13 April 2023

Accepted: 17 April 2023

Published: 20 April 2023



**Copyright:** © 2023 by the authors. Licensee MDPI, Basel, Switzerland. This article is an open access article distributed under the terms and conditions of the Creative Commons Attribution (CC BY) license (<https://creativecommons.org/licenses/by/4.0/>).

## 1. Introduction

Water stress is a pressing issue that affects many regions of the world, particularly in arid and semi-arid areas where water resources are scarce. In recent years, governments and humanitarian organizations have attempted to address this issue by improving access to water for those living in water-stressed areas. However, as climate change and population growth continue to pressure water resources, the problem is expected to worsen in the coming years. In addition, water stress can impact agricultural production, which can have an effect on the economy and food security [1,2]. Water stress can result in conflicts and mass migrations in certain cases. Moreover, the migration of people due to water stress can pose

new challenges for governments and humanitarian organizations. Mitigating the challenges associated with water stress necessitates a collective endeavor from all stakeholders. Global collaboration in water management, in conjunction with efficacious policies and practices at the regional level, can facilitate the provision of secure and hygienic water access for all, and avert the societal, economic, and ecological repercussions stemming from water stress [3]. Countries are being encouraged to implement innovative and sustainable measures such as rainwater harvesting and enhanced irrigation techniques [2]. The Middle East has faced a severe water scarcity problem in recent decades due to climate change and inadequate management of water resources [4,5]. Water scarcity considerably limits wheat production in Northern Iraq, especially in regions with low and erratic rainfall during the crop growth period. In such circumstances, supplemental irrigation can boost and sustain yields over time, particularly if applied during critical growth stages [6].

Supplementary irrigation has been identified as a plausible measure to address this quandary. This entails the provision of supplementary water by farmers to their crops to offset the shortfall in precipitation, especially during crucial growth phases, since wheat necessitates varying quantities of water at distinct stages of its growth. The application of supplementary irrigation at vital growth stages warrants the provision of adequate water supply to the crop during its peak water requirements, and thereby augments and preserves yields over a protracted time period, even in regions confronted with a dearth of or erratic precipitation [1,7].

The inaccessibility of sufficient water resources can pose a formidable obstacle to farmers, particularly during periods of drought [8]. Shallow and deep tube wells are both employed as means to provide irrigation water. In 2007, the Ministry of Agriculture and Water Resources of the KRI initiated a program to assist farmers with contemporary irrigation systems, such as the center pivot, to enhance crop production after experiencing droughts on several occasions in previous years. Nevertheless, inadequate awareness regarding water scarcity and efficient water utilization has led some farmers to utilize the center pivot for prolonged durations and over-irrigate by extending the center pivot revolution time to amplify the water application depth. The assimilation of crop models and remotely sensed data via optimization algorithms has emerged as an efficacious and prospective technique for monitoring crop growth status and appraising crop yields, as it ameliorates specific deficiencies and amalgamates the benefits of individual methods [9,10].

In the KRI region, groundwater is abundant and generally of reasonable quality, but it has been heavily extracted for domestic, agricultural, and industrial purposes, resulting in a depletion of the groundwater table level. Mitigating the effects of climate change and rehabilitating nature requires more water management projects to ensure the efficient use of available water. Groundwater is the primary source of inaccessible surface water, and rainfall, groundwater, and rivers account for 51%, 48%, and 1% of crop production water, respectively [11]. Despite an increasing number of wells and groundwater abstraction in the Erbil plain, the aquifer is being harmed, with an average drop in groundwater levels of 50 m [2].

Agriculture is the largest water-consuming sector globally, accounting for 78–90% of water use, followed by domestic and industrial use [12]. In Iraq, the agricultural sector is the primary consumer of water resources. Irrigation in Iraq relies on three main sources of water: surface water, rainwater, and groundwater, and farmers use drip, sprinkler, and central pivot irrigation techniques [13]. Wheat and barley are the dominant crops in Iraq, covering 73% of the total cultivated land [14]. Wheat productivity under irrigation exceeds rainfed productivity by a factor of two to three, demonstrating the high productivity potential of wheat varieties under irrigation [2]. Given the increasing scarcity of freshwater, it is critical to optimize water use, particularly in irrigated agriculture [15]. Rainfall is the primary source of water for agriculture in Iraq, accounting for 51% of water supply during winter, while groundwater and rivers contribute 48% and 1%, respectively [16], as per the joint report of UNDP, USAID, and FAO (2019). Farmers in arid regions are confronted with a multitude of challenges, such as low agricultural productivity, frequent droughts, climate

variability, high soil erosion rates, and deforestation [17]. Nevertheless, a comprehensive study of drought must be conducted for each area to develop a research framework [18,19]. Understanding the spatial and temporal variations in crop growth is crucial for effective crop management and achieving food security. The combination of remote sensing data and crop growth models has proven to be a valuable approach for monitoring crop growth and estimating crop yields.

The impact of climate change, combined with reduced water discharge in the Tigris and Euphrates rivers, has led to more frequent droughts in Iraq, which have particularly affected agriculture, resulting in significant reductions in crop yields and vegetation cover [20]. The Erbil province, KRI, is particularly vulnerable to severe drought, with reports indicating a reduction in precipitation and vegetation cover in 2000, 2008, 2012, and 2021 [21,22]. Southern and western parts of the KRI have been the hardest hit by rainfall shortages, whereas the north and east have seen increased moisture levels. The FAO has predicted that wheat crop production in northern Iraq will be approximately 50% lower in 2021 than the previous year, according to KRI authorities [8,23]. The use of secondary agricultural data in combination with remote sensing can provide more accurate estimates of irrigation performance [24]. The NDVI is a useful parameter for crop monitoring due to its unambiguous response to irrigation interventions. Modern irrigation management strategies aim to enhance agricultural productivity while minimizing water consumption [25], which is crucial given the limited water supply in changing environmental conditions. The NDMI can be used to describe a crop's water stress level and is calculated as the ratio between the difference and the sum of the refracted radiation in the near-infrared and SWIR spectrums [26]. Effective water resource management and enhancement of water productivity require a sound understanding and management of evapotranspiration [27]. Monitoring significantly varying Normalized Difference Vegetation Index (NDVI) values in a region can provide valuable insight into potential pest or disease concerns and the presence of weeds in areas of a field [28]. NDVI data can be used to display changes in vegetation cover and analyze patterns of drought occurrences. However, the performance of NDVI may be influenced by mistakes during the growing season and saturation effects on dense vegetation [29]. Therefore, additional factors should be considered to improve the precision of the results [30]. Various alternative vegetation and moisture indices are available to monitor crop growth, including the Enhanced Vegetation Index (EVI), Normalized Difference Water Index (NDWI), Leaf Area Index (LAI), Soil Adjusted Vegetation Index (SAVI), Thermal Vegetation Index (TVI), Crop Water Stress Index (CWSI), and Temperature Vegetation Dryness Index (TVDI). The most appropriate index selection depends on various factors, such as the type of crop, growth stage, and environmental conditions. NDVI have been widely used in semi-arid areas and have shown good performance in detecting vegetation changes [31–33]. The Normalized Difference Moisture Index (NDMI) is a reliable indicator of vegetation water content and can be used to monitor water stress in crops or other vegetation, particularly in areas where water stress is a concern [34,35]. NDMI is derived from the difference between the near-infrared and mid-infrared bands of satellite imagery. By monitoring NDMI values over time, changes in vegetation water content can be detected and the level of water stress experienced by crops or other vegetation can be assessed [15].

Inefficient water application occurs when the irrigation system is not appropriately managed, resulting in uneven water distribution across the field, reduced crop yields, and soil erosion. Such inefficiency happens when water evaporates or is lost through other means. Minimizing water loss requires proper irrigation scheduling, use of efficient irrigation systems, and managing the system appropriately based on remote sensing. Monitoring through the Sentinel satellite every five days and ETo, ETc data helps ensure proper irrigation scheduling based on remote sensing and GIS techniques. The capability to develop agriculture effectively with limited water resources is a crucial strategic objective for addressing future climate change and fulfilling Sustainable Development Goal 2 of the United Nations (SDG2). The primary objective of this research is to comprehend the impact

of drought and compare wheat production between rainfed and center pivot systems during the study period. Additionally, it seeks to analyze the key factors that affect the spatial and temporal variation of NDVI and NDWI in wheat cultivated on center pivots. The study aims to investigate irrigation performance and water productivity at various scales to develop suitable water management strategies, especially considering decreasing water availability, rising threats from climate change, and growing population and food demand. This study provides a new strategy for agricultural resource management by providing consistent estimations of winter wheat water requirements and yield. This information can be used to optimize irrigation practices and improve crop management, particularly in arid and semi-arid regions where water availability is limited.

## 2. Materials and Methods

### 2.1. Study Area

The study area, comprising the Ain Kawa sub-district in the Erbil Governorate of northern Iraq, is illustrated in Figure 1 and spans an estimated area of 25,525 hectares. North Erbil was chosen as the case study region for a combination of reasons. Firstly, the wheat, which is a crucial crop that contributes significantly to the Kurdistan Region of Iraq's economy, is extensively grown in the region. Secondly, Erbil is a vital agricultural center, known as Iraq's breadbasket, and is responsible for a substantial portion of the country's food supply. Finally, the need to enhance and expand the existing water management sector in Iraq is pressing, and there are related challenges that require immediate attention.

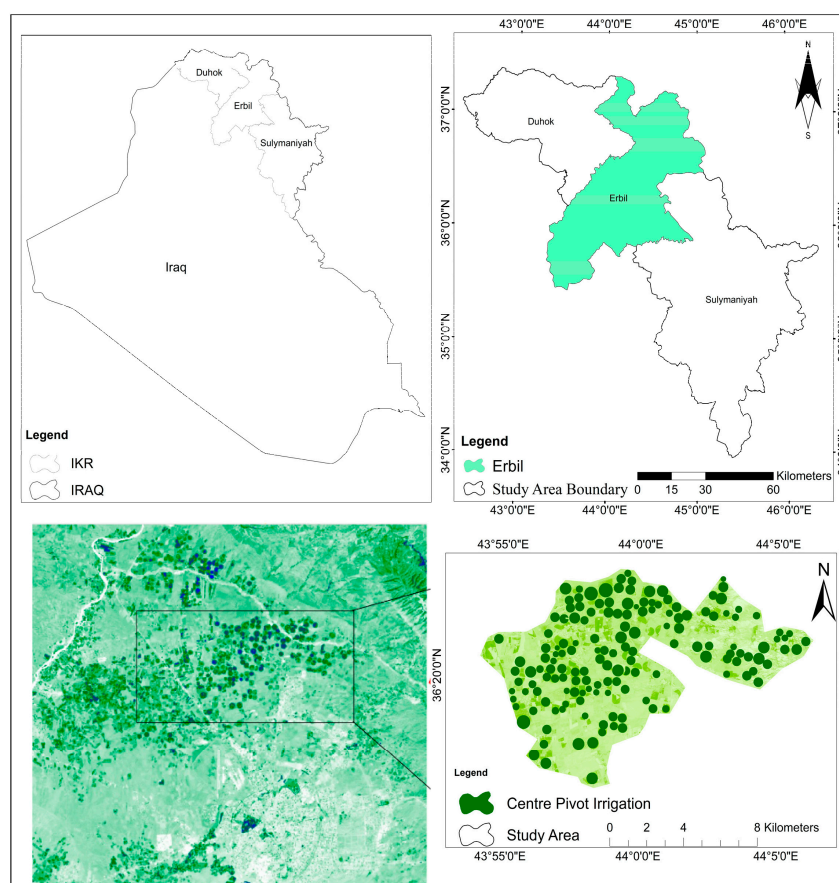


**Figure 1.** Site map of the study area in Erbil, KRI.

### 2.2. Climate

The climatic conditions prevailing in Erbil, KRI, are predominantly continental, sub-tropical, and semi-arid, while a Mediterranean climate characterizes the mountainous parts. Rainfall in the mountainous areas usually occurs between December to February or Novem-

ber to April. The average daytime temperature during winter is approximately 16 degrees Celsius, which drops to around 2 °C at night, with a possibility of frost. Conversely, summers are characterized by high temperatures, with an average temperature exceeding 45 °C in July and August and falling to around 25 °C at night [36,37]. The period of precipitation in the region is typically between October to May, with the annual rainfall ranging between 100 and 200 mm. The Ministry of Agriculture and the Department of Meteorology in the KRI have validated the accuracy of the average precipitation recorded during this period. It is worth noting that farmers in the study region rely on rainfall to irrigate their crops, although they often supplement it with irrigation to enhance crop productivity.

#### Meteorological Data

Figure 2 presents the data on the mean daily maximum and minimum temperature, relative humidity, wind speed, sunshine, and hours, collected from the Ministry of Agriculture and Water Resources of Erbil for two stations during the year 2021.

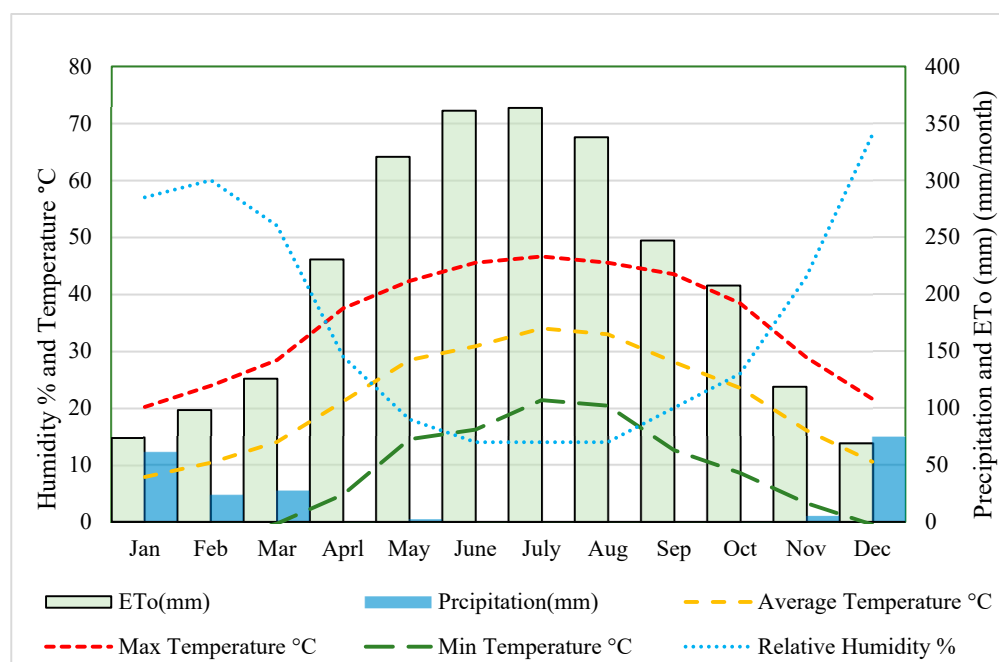


**Figure 2.** Monthly precipitation, relative humidity, actual evaporation, maximum, minimum, and mean temperature of North Erbil and surrounding areas recorded for 2021 years.

#### 2.3. Sentinel 2 Satellite Imagery Acquisition

This study used open-access satellite data from the Sentinel 2 missions to calculate the vegetation and water indices as a proxy for factors. Sentinel-2 is a 10 m high-resolution, wide-swath, multispectral imaging mission that supports Copernicus Land Monitoring investigations, such as plant, soil, and water cover monitoring, and observation of both inland waterways and coastal regions [38]. Thirteen spatial resolution spectral bands captured by Sentinel-2 represent TOA reflectance, including four bands at 10 m, six at 20 m, and three at 60 m spatial resolution. In addition to data from the Sentinel 2 missions, detailed meteorological and secondary data from the literature were required, including corn winter wheat crops for monthly, seasonal periods in 2021, with season intervals ranging from January to May. The Copernicus Open Access Hub was used for this investigation to obtain Level-1C products of Sentinel-2 A/B satellite data. These products contain top-of-atmosphere (TOA) reflectance values for 13 spectral bands with spatial resolutions ranging from 10 to 20 m. The Sentinelsat Python API was used to obtain the data for the study area and time period of interest, which were subsequently preprocessed in Google Earth Engine (GEE) to acquire surface reflectance values. The preprocessing procedure involved

resampling the data to a standardized spatial resolution of 10 m, masking out clouds and cloud shadows utilizing the SCL band, and applying a bi-directional reflectance distribution function (BRDF) correction to consider the impact of directional effects induced by surface roughness and slope.

In order to enable more in-depth analysis and visualization, the classified Sentinel 2 data underwent a process of division into smaller tiles. This was accomplished utilizing the `ee.data.getTileUrl` function in the GEE cloud-based platform, which allowed the extraction of individual tiles based on their geographical coordinates and zoom level. The resulting tiles were then saved in the GeoTIFF format, which can be easily imported into QGIS and other GIS software for further processing and analysis. The classified and divided Sentinel 2 data were subsequently subjected to a range of statistical analyses, including frequency distributions, cross-tabulations, and spatial autocorrelation analysis, which were performed using both GEE and QGIS software. These analyses were employed to quantify the spatial patterns and relationships between different meteorological variables in the study area. Additionally, it is imperative to comprehend the current status of the center pivot’s performance for the purpose of determining its potential for improvement. As such, a manual selection process was undertaken, which involved identifying 143 center pivot farms in the vicinity for further investigation.

The biophysical factors were computed using the formula derived from Sentinel 2 Indices, which comprises two satellite sensors (S2A and S2B) that have generated products with a 5-day temporal resolution (at the equator) and a 10 m spatial grid-cell resolution since January 2021. The satellite products from the Sentinel 2 mission were obtained and analyzed using GEE. The QGIS (v 24.3) geographic information system program utilized the Semi-Automatic Classification Tool plugin, with the following options defined in the plugin’s menu: (a) Band 4-RED and Band 8-NIR from Sentinel 2; (b) the study area coordinates; (c) the time search windows from 1 January to 21 May in 2021, as well as (Figure 3); and (d) an acceptable imagery cloud cover set to 100%. Figure 1 illustrates a Google Earth satellite image of a farm utilizing a center-pivot irrigation system in the study area.

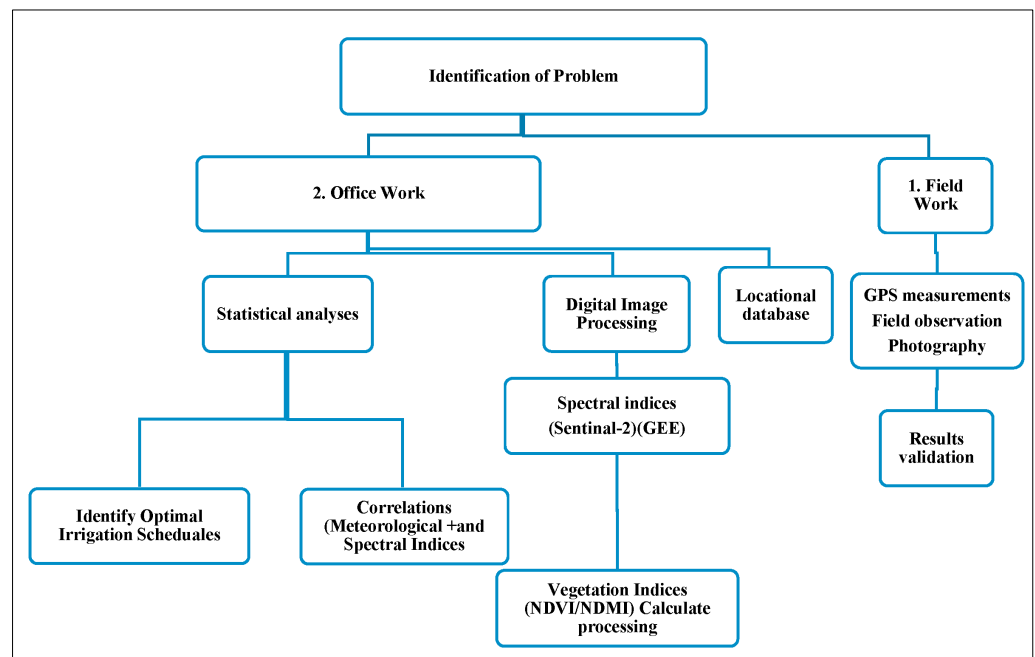


Figure 3. Flowchart of the methodology adopted in this study.



### 2.5.2. NDMI

The NDMI normalizes the different moisture response bands between near-infrared (NIR) and shortwave infrared (SWIR) (Equation (2)). The linear correlation between the NIR/SWIR ratio and leaf relative water content was discovered by Hunt Jr and Rock [41]. He calculated NDMI using the following equation:

$$\text{NDMI} = \frac{\text{NIR} - \text{SWIR}}{\text{NIR} + \text{SWIR}} \quad (2)$$

where NIR is the Near-Infrared band and SWIR is the Shortwave Infrared band. The values of these bands can be obtained from remote sensing data, such as satellite imagery.

The NDMI ranges from  $-1$  to  $1$ , where values closer to  $1$  indicate high moisture content in vegetation, and values closer to  $-1$  indicate low moisture content. In general, vegetation with high moisture content reflects more NIR and absorbs more SWIR, resulting in a higher NDMI value. NDMI is often used in agriculture and environmental monitoring to assess vegetation health and drought conditions. It can be used to detect areas of vegetation stress, monitor changes in soil moisture, and predict crop yields [41].

### 2.6. Meteorological Indices

Reference Evapotranspiration (ET<sub>o</sub>), and Crop Evapotranspiration (ET<sub>c</sub>)

The FAO Penman–Monteith equation is a close, simple representation of the physical and physiological factors governing the evapotranspiration process. Using the FAO Penman–Monteith definition for (ET<sub>o</sub>), the formula for ET<sub>o</sub> using the Penman–Monteith equation is:

$$\text{ET}_o = \frac{0.408 \times \Delta \times R_n + \gamma \times (900 / (T + 273)) \times U_2 \times (e_s - e_a)}{\Delta + \gamma \times (1 + 0.34 \times U_2)} \quad (3)$$

where:

ET<sub>o</sub> = potential evapotranspiration (mm/day).

Δ = slope of the saturation vapor pressure-temperature curve (kPa/°C).

R<sub>n</sub> = net radiation at the crop surface (MJ/m<sup>2</sup>/day).

T = mean daily air temperature at 2 m height (°C).

U<sub>2</sub> = wind speed at 2 m height (m/s).

e<sub>s</sub> = saturation vapor pressure (kPa).

e<sub>a</sub> = actual vapor pressure (kPa).

γ = psychrometric constant (kPa/°C) [42].

Crop evapotranspiration (ET<sub>c</sub>) is the amount of water lost from a crop due to evaporation from the soil surface and transpiration from the crop itself. It is a measure of the amount of water required for a specific crop to achieve optimum growth and yield. Various factors, including the climate, soil characteristics, crop type, and stage of growth, influence ET<sub>c</sub>. The most common method used to estimate ET<sub>c</sub> is using reference evapotranspiration (ET<sub>o</sub>), which is the amount of water lost from a reference crop under standardized conditions. Once the ET<sub>o</sub> is calculated, crop coefficients are applied to adjust the ET<sub>o</sub> for the specific crop being grown [42].

The resulting value is the crop evapotranspiration (ET<sub>c</sub>) for that crop at that location and time. ET<sub>c</sub> is an important parameter in irrigation management, as it determines the amount of water that must be applied to a crop to maintain optimal growth and yield. Over-irrigation can lead to waterlogging and the leaching of nutrients, while under-irrigation can reduce crop yield and quality. Therefore, an accurate estimation of ET<sub>c</sub> is crucial for the efficient and sustainable use of water resources in agriculture [42]. The ET<sub>c</sub> equation is expressed as:

$$\text{ET}_c = K_c \times \text{ET}_o \quad (4)$$

where:

ET<sub>c</sub> = crop evapotranspiration (mm/day).

K<sub>c</sub> = crop coefficient (dimensionless).

$E_{To}$  = potential evapotranspiration (mm/day) [42].

### 3. Results and Discussion

#### 3.1. NDVI and NDMI

Based on remote sensing data, the NDMI values show more pronounced changes between February and March, potentially due to local farmers perceiving irrigation as unnecessary during January and February's cold weather. The higher variability in NDMI values indicates that it responds to changes in soil moisture content. Similarly, the greater vertical variability in biomass suggests that wheat biomass reacts more significantly to moisture stress during the initial growth stage (February). This implies that crops are more vulnerable to stress in March and April than in other months. A comparison of NDVI- and NDMI-designated fields indicates that irrigation's impact on crop yield varies geographically, with a substantial yield increase observed in areas with abundant light. To maximize yield, it is crucial to avoid water stress during the wheat's most susceptible seasons. However, there was a moderately negative correlation between NDVI and NDMI in 2021. Moreover, the majority of hotspot fields exhibited higher NDMI values, while bright spots showed early growth and greater biomass accumulation throughout the growing stages. This difference may be related to irrigation methods and soil moisture stress, particularly in March and April when the center pivot is essential for reducing temperature and relieving soil moisture stress. However, some farmers do not irrigate during January and February, which may lead to water stress. Remote sensing can detect the effects of water stress on plants with a lag time.

The NDVI has been widely used to investigate the correlation between spectral vegetation variability and growth rate changes. The findings of this investigation have demonstrated that the NDVI values fluctuated between 174.5 area/ha in January, the lowest area of dense NDVI, and 6028.3 ha in April, the highest area. The NDVI Value is a numerical index employed to assess vegetation health and growth. It indicates denser and healthier vegetation, with higher values ranging from  $-1$  to  $+1$ . The NDVI value categorizes vegetation density into different classes such as Dense, Moderate, Sparse, and Open vegetation. The area of each category is measured in hectares (ha), a common unit in agriculture. Table 1 shows the NDVI Area/ha for Dense Vegetation Classes for different months, which include 1-Jan, 6-Jan, 11-Jan, 26-Jan, 15-Feb, 25-Feb, 7-Mar, 1-Apr, 11-Apr, 16-Apr, 21-Apr, 1-May, 6-May, 11-May, 16-May, and 21-May. The values of the NDVI area/ha for the Dense category during those months are 1174.49, 386.00, 372.47, 549.33, 3191.68, 4536, 5334.15, 6028.25, 3850.27, 3327.33, 2362.02, 1789.78, 1702.87, 801.12, 171.77, and 58.61, respectively. The Dense category signifies areas with high vegetation density, indicating the presence of very healthy vegetation.

According to the data presented in Table 1, there was a noticeable change in the vegetation status of the Center pivot area from January to May. Specifically, the NDVI value of the Center pivot area decreased significantly in May due to the maturity stage of the crops and the increase in  $E_{To}$ , which resulted in a reduction in the agricultural land area. Moreover, the rise in temperature was detectable earlier, particularly during the drought season. Thus, NDVI with NDMI can help improve our understanding of how irrigation and climate change affect the yield and can be used as an early warning for Moisture stress. Moreover, this information can assist farmers and policymakers in making more informed management decisions. In order to achieve the greatest range of NDVI and NDMI values for wheat crops in 143 central pivot areas in north Erbil, we utilized Sentinel 2 images on coincident days. The dataset used for NDVI and NDMI was then split into two subsets: a training dataset and a validation dataset. These datasets were collected from 1 January 2021 to 21 May 2021, covering fourteen Center pivot areas throughout the phenological cycle to monitor various crops. The analysis of Tables 1 and 2 and Figures 5 and 6 revealed that the study region experienced drought episodes over the study period, with March and April 2021 being particularly affected.

**Table 1.** Statistical indices of measured NDVI value, classes density, and area of each class.

Vegetation Classes	1-Jan-21	6-Jan-21	11-Jan-21	26-Jan-21	15-Feb-21	25-Feb-21	7-Mar-21	1-Apr-21
DENSE	0.60–1.00	0.60–1.00	0.60–1.00	0.60–1.00	0.60–1.00	0.60–1.00	0.60–1.00	0.60–1.00
Area/ha	174.49	386.00	372.47	549.33	3191.68	4536	5334.15	6028.25
MODERATE	0.40–0.60	0.40–0.60	0.40–0.60	0.40–0.60	0.40–0.60	0.40–0.60	0.40–0.60	0.40–0.60
Area/ha	411.69	1294.53	1171.53	2028.78	3269.82	3154.02	3043.28	2296.82
SPARCE	0.20–0.40	0.20–0.40	0.20–0.40	0.20–0.40	0.20–0.40	0.20–0.40	0.20–0.40	0.20–0.40
Area/ha	3601.15	5261.86	4639.91	4554.1	2880.12	1410.72	1161.43	762.6
OPEN SOIL	–1.00–0.20	–1.00–0.20	–1.00–0.20	–1.00–0.20	–1.00–0.20	–1.00–0.20	–1.00–0.20	–1.00–0.20
Area/ha	5055.9	3031.05	3182.37	1495.82	664.35	542.26	443.31	481.79
Vegetation Classes	11-Apr-21	16-Apr-21	21-Apr-21	1-May-21	6-May-21	11-May-21	16-May-21	21-May-21
DENSE	0.60–1.00	0.60–1.00	0.60–1.00	0.60–1.00	0.60–1.00	0.60–1.00	0.60–1.00	0.60–1.00
Area/ha	3850.27	3327.33	2362.02	1789.78	1702.87	801.12	171.77	58.61
MODERATE	0.40–0.60	0.40–0.60	0.40–0.60	0.40–0.60	0.40–0.60	0.40–0.60	0.40–0.60	0.40–0.60
Area/ha	2825.15	1535.55	1229.22	295.54	708.61	1184.93	409.53	126.65
SPASE	0.20–0.40	0.20–0.40	0.20–0.40	0.20–0.40	0.20–0.40	0.20–0.40	0.20–0.40	0.20–0.40
Area/ha	2787.42	3660.23	4406.41	919.25	1600.48	2179.02	2961.71	2577.09
OPEN SOIL	–1.00–0.20	–1.00–0.20	–1.00–0.20	–1.00–0.20	–1.00–0.20	–1.00–0.20	–1.00–0.20	–1.00–0.20
Area/ha	442.22	626	763.32	1662.93	4208.1	5691.78	6222.15	7201.58

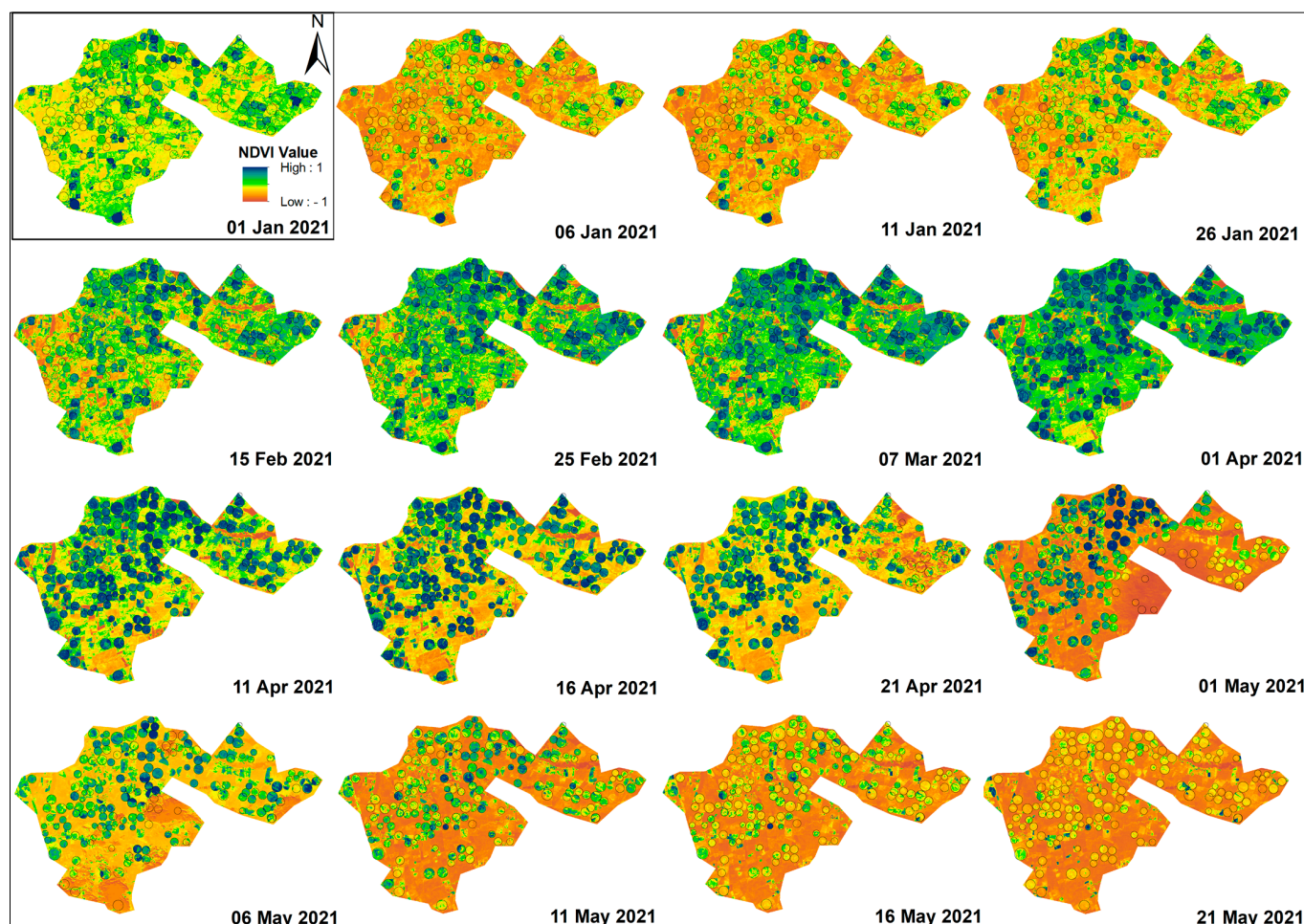


**Figure 5.** Temporal Variation of the NDVI Value-Based Vegetation Density Classes of Wheat Field in 2021.

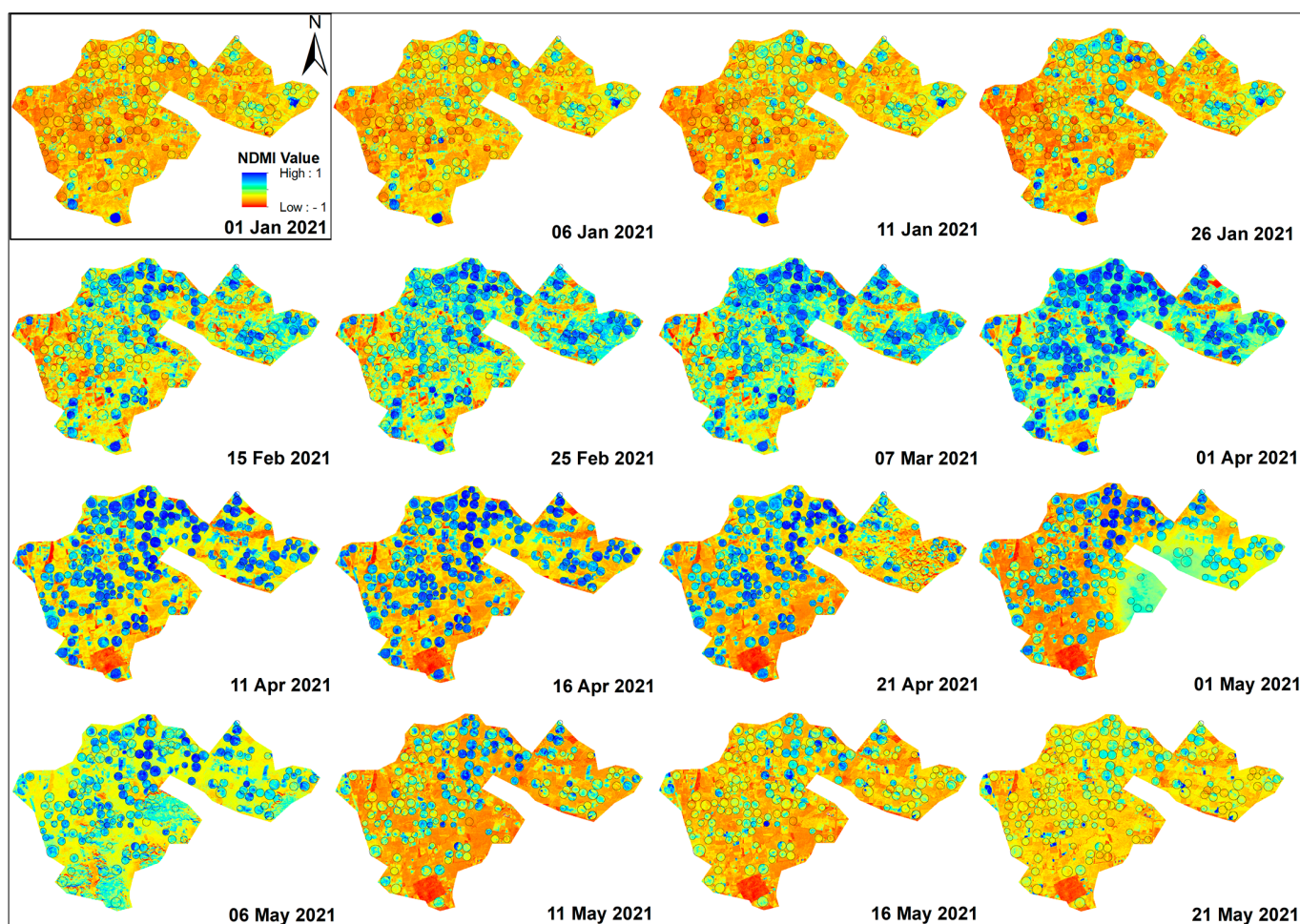


Figure 6. Temporal Variation of the NDMI Value-Based Vegetation Density Classes of Wheat Field in 2021.

Table 2. Statistical indices of measured NDMI Value, and area of each Classes.

NDMI Classes	1-Jan-21	6-Jan-21	11-Jan-21	26-Jan-21	15-Feb-21	25-Feb-21	7-Mar-21	1-Apr-21
HIGH	0.50–1.00	0.50–1.00	0.50–1.00	0.50–1.00	0.50–1.00	0.50–1.00	0.50–1.00	0.50–1.00
Area/ha	0.28	1.68	3.72	0.04	65.96	115.88	239.64	337.28
MODERATE	0.30–0.50	0.30–0.50	0.30–0.50	0.30–0.50	0.30–0.50	0.30–0.50	0.30–0.50	0.30–0.50
Area/ha	63.12	90.56	95.48	184.76	1618.2	2329.76	2961.12	3515.56
LOW	0.10–0.30	0.10–0.30	0.10–0.30	0.10–0.30	0.10–0.30	0.10–0.30	0.10–0.30	0.10–0.30
Area/ha	354.76	667.24	779.72	1700.92	3576.84	4301.56	4486.52	4859.68
OPEN SOIL	0.00––1.00	0.00––1.00	0.00––1.00	0.00––1.00	0.00––1.00	0.00––1.00	0.00––1.00	0.00––1.00
Area/ha	9563.54	9250.72	7202.48	3567.1	4781.4	3066.52	2331.81	921.62
NDMI Classes	11-Apr-21	16-Apr-21	21-Apr-21	1-May-21	6-May-21	11-May-21	16-May-21	21-May-21
HIGH	0.50–1.00	0.50–1.00	0.50–1.00	0.50–1.00	0.50–1.00	0.50–1.00	0.50–1.00	0.50–1.00
Area/ha	877.52	979.24	5.12	367.44	37.7	5.48	2.52	1.84
MODERATE	0.30–0.50	0.30–0.50	0.30–0.50	0.30–0.50	0.30–0.50	0.30–0.50	0.30–0.50	0.30–0.50
Area/ha	2616.08	2125.84	2313.64	1187.68	1005.96	594.6	86.76	40.36
LOW	0.10–0.30	0.10–0.30	0.10–0.30	0.10–0.30	0.10–0.30	0.10–0.30	0.10–0.30	0.10–0.30
Area/ha	3554.6	1700.84	1850.08	1024.64	1647.48	1840.68	361.7	489.92
OPEN SOIL	0.00––1.00	0.00––1.00	0.00––1.00	0.00––1.00	0.00––1.00	0.00––1.00	0.00––1.00	0.00––1.00
Area/ha	2968.74	3588.14	4579.58	671.2	5759.16	2529.62	8867.86	9504.2

Table 1 shows the correlation between drought and reduced vegetation area/NDVI mean values, further supporting the importance of water availability for vegetation growth. It is also possible that other factors, such as temperature and nutrient availability, may contribute to the observed differences in vegetation indices between the two fields. There

is a clear difference in the vegetation indices (NDVI and NDMI) between the irrigated and rain-fed fields during the growing season months of March and April. The irrigated field shows a significant change in NDVI values and NDMI, which may indicate increased vegetation growth due to water availability. On the other hand, the rain-fed field experiences drought during these months, which is correlated with reduced vegetation area and lower NDVI mean values. It is worth noting that NDVI is a commonly used index for evaluating the health and growth of vegetation, as it quantifies the chlorophyll content in plant leaves. On the other hand, NDMI is an indicator of vegetation water content and can offer insights into soil moisture conditions [7].

Consequently, the observed dissimilarities in NDVI and NDMI values between irrigated and rain-fed fields imply that water availability is a crucial determinant of vegetation growth and productivity. Nonetheless, it was observed that NDMI values increased significantly during the months of March and April, especially in the irrigated field, when the crops were subjected to 72 to 96 h of irrigation per month. In contrast, the NDVI value showed very little vegetation, particularly in the non-irrigated section of the study area (see Figures 5 and 6).

These findings are consistent with those of a previous study by [43]. The temporal fluctuations in NDVI and NDMI demonstrated that the drought resulted in a decline in the value and extent of spectral indices from normal to extreme levels, with the non-irrigated area being the driest. Conversely, the field where supplementary irrigation was applied during the specified period had high NDVI coverage. The NDVI values revealed that the non-irrigated area in the study region was affected by drought (see Figures 5 and 6). However, the severity and spatial extent of the drought varied. Low values indicated a dry season, whereas high values indicated a wet season [44]. From January to May, the NDVI values exhibited temporal and spatial variations across the region (Figures 5 and 6), primarily attributed to differences in precipitation amount, frequency, and intensity [45]. Moreover, meteorological factors such as precipitation, temperature, and relative humidity were crucial in influencing NDVI variability [46]. The spatial variability of NDVI values was determined by several factors, including climate, soil, temperature, ETo, and ETc fluctuations (refer to Table 3).

**Table 3.** The fourteen fields were monitored during five months of irrigation, with irrigation hours used for each center pivot by month.

Location	Longitude	Latitude	Yield Kg/ Hectare	Irrigation/h/mm							
				January	February	March	April	May	Total/ Hours	Mm/ Hours	Mm/ Season
1	43.96674	36.35929	3120	24	48	72	72	18	234	2.1	491.4
2	43.96334	36.36667	3400	36	48	86	72	18	260	2.1	546.0
3	43.96235	36.37074	3320	24	36	72	72	12	216	2.1	453.6
4	43.96983	36.37265	2960	24	48	72	72	12	228	2.1	478.8
5	43.97896	36.37460	3520	36	48	96	96	6	282	2.1	592.2
6	43.98112	36.36880	3360	24	48	72	80	6	230	2.1	483.0
7	43.98278	36.36585	3400	12	48	72	72	12	216	2.1	453.6
8	43.97472	36.37033	3400	12	36	72	80	12	212	2.1	445.2
9	43.97036	36.36933	3800	24	48	72	72	12	228	2.1	478.8
10	43.97635	36.36438	4800	24	48	96	96	12	276	2.1	579.6
11	43.97226	36.36283	3520	18	36	72	80	6	212	2.1	445.2
12	43.97428	36.36111	4400	24	48	72	96	24	264	2.1	554.4
13	43.95905	36.28151	5000	24	48	76	96	12	256	2.1	537.6
14	43.97158	36.28487	4800	36	48	76	96	18	274	2.1	575.4

The NDMI is a remote sensing metric used to measure how much water is in vegetation. Higher values mean that the vegetation has more water. Such areas may be irrigated or have access to other sources of water. The NDMI values for certain months and areas. Larger values mean that plants are especially healthy because there is a lot of water. Specifically,

NDMI values for the High Values category in the months of January through May. The values for this category are 0.28, 1.68, 3.72, 0.04, 65.96, 115.88, 239.64, 337.28, 877.52, 979.24, 5.12, 367.44, 37.7, 5.48, 2.52, and 1.84, respectively. High Values in the table indicate areas with abundant water in the vegetation, which signifies particularly healthy vegetation. Both the NDVI and the NDMI are commonly used as remote sensing indices to measure how healthy plants are and how much water they have. This information could be used to improve irrigation efficiency and determine how much water plants need based on satellite data. NDVI is typically used to estimate crop yield, vegetation cover, and photosynthetic activity. In this study, NDVI was used to find plants that were water stressed, which is a common problem in agriculture that uses water. Farmers can improve irrigation schedules, increase crop yields, and waste less water by keeping an eye on NDVI values.

The NDMI index is utilized for the estimation of soil moisture and water stress in crops, and it can aid farmers in adjusting their irrigation schedules to optimize water usage and improve crop yield. Changes in NDVI and NDMI values prior to and following irrigation can assist farmers in gauging the amount of water required to attain the desired vegetation growth or moisture content. The NDMI values were observed to be at their minimum during January and May, indicating reduced vegetation and lower NDVI values (Figures 5 and 6), which could be attributed to decreased rainfall during those months. However, during February, March, and April, NDMI values increased, which was positively correlated with the application of supplementary irrigation, suggesting that irrigation had a beneficial impact on vegetation growth during these months. The decline in NDMI values during the growth season could be attributable to the adverse effects of high temperatures on vegetation growth. The study area witnessed a significant decrease in annual rainfall averages, which could have impacted overall vegetation growth. The 14 fields received 445.2 mm and 579.6 mm of irrigation water, respectively.

During the 2021 monitoring season, irrigation amounts were measured in Fields C1 to C14 using a water meter, which recorded a total of 350 mm of water. One or two irrigation events were performed during the early growing stage to ensure the establishment of robust young plants. Subsequently, irrigation for Fields C1 to C14 was scheduled based on NDMI sensor measurements to irrigate when the depletion level within the rooting zone was ready to drop 60% of the total available below. An algorithm was executed with a crop file created based on Fields measurements and observations and dynamically modified during the cultivation season by adjusting weather parameters. Field-specific constraints, such as not allowing irrigation events to occur more often than once every four days, were integrated into the scheduling process. In cases where the generated irrigation schedule was not followed (e.g., due to an electrical failure in the pumping station or damage to the irrigation system), the algorithm was re-executed, and the irrigation schedule was adjusted accordingly. Despite these adjustments, consistent violations of the first depletion threshold occurred, as irrigation was applied either before the threshold was reached or after the water content had fallen below it.

In dryland areas, supplemental irrigation is often necessary to support crop growth, especially during the winter months from January to May. The region employs various irrigation technologies, including Center pivot irrigation and homogeneous irrigation systems. Monitoring vegetation variability using central pivots is feasible, and the NDMI is a useful input variable for irrigation prediction models, as it correlates with the NDVI, which is considered moderate in Center Pivot techniques (as demonstrated in Figures 6 and 7). It is crucial to validate modeling results to ensure their reliability. Figure 8 shows low variability, indicating that the modeling approaches used in this study were robust. The study utilized a combination of remote sensing techniques and meteorological data to evaluate the efficacy of irrigation systems, and the results indicated that this approach was reliable and robust. Remote sensing was employed to collect data on the water supply to crops and its impact on crop growth, while meteorological data provided information on weather patterns, including precipitation, temperature, humidity, ETo, and ETc, which affected crop growth and irrigation needs. The integration of these two data types enabled

the development of a comprehensive model for assessing irrigation system performance. The study found that this approach was effective in providing accurate information about the system’s performance, which could help optimize irrigation methods and enhance crop yields.

Notably, all methodologies employed in this study were linear based. Ideally, a well-designed irrigation system would ensure uniform water distribution, which would result in homogeneous water consumption patterns across fields. However, several factors, including deficient infrastructure, inadequate management practices, soil type, water quality, and fertilization, can lead to non-uniform water use across fields and zones. The amount of irrigation water applied in each event was measured through the use of rain gauges positioned above the crop canopy (see Figures 7 and 8). This methodology was proposed and implemented by María [47].

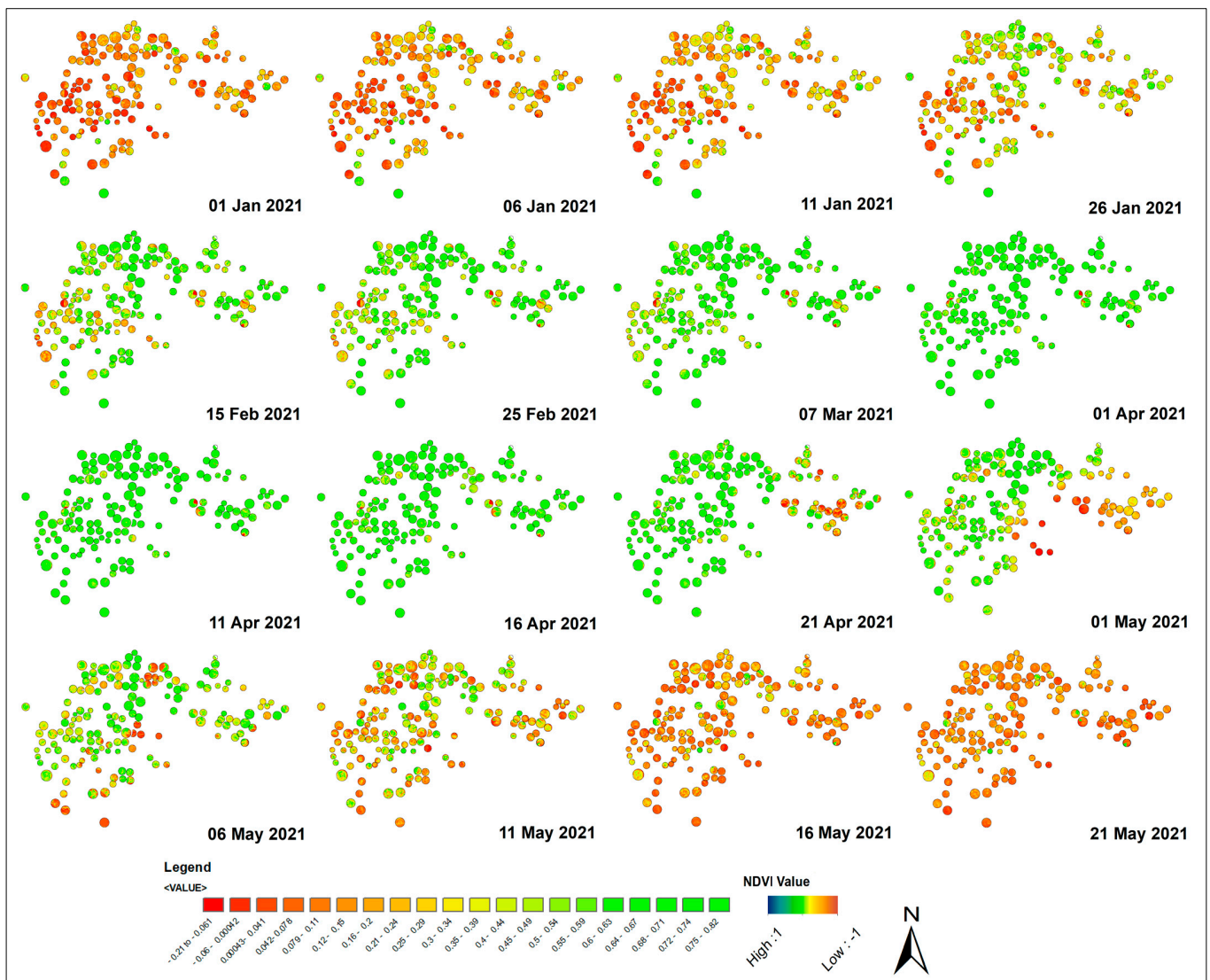
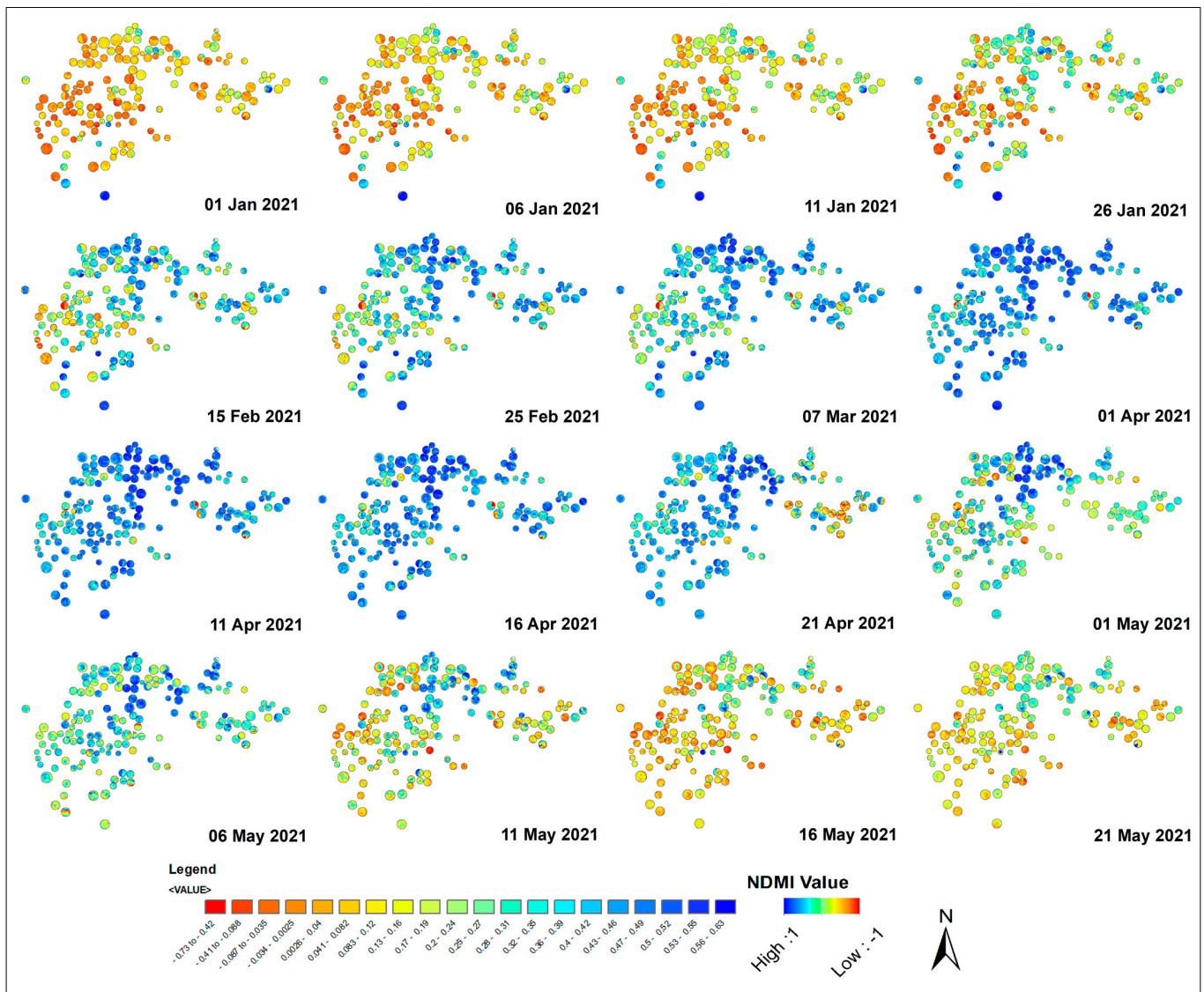


Figure 7. Temporal Variation of the NDVI Value of Centre pivot fields in 2021.



**Figure 8.** Temporal Variation in the NDMI Value of Center pivot fields in 2021.

### 3.2. Crop Water Use and Water Use Efficiency

During the period from January 2021 to May 2021, a total of 14 Center pivot (C) fields were subjected to rigorous monitoring to ascertain their irrigation schedules, crop growth, and soil moisture profiles, enabling the assessment of water productivity. The irrigation schedules were established by the farmers, who relied on weather forecasts to optimize their plans. In this regard, the irrigation plan was adjusted to compensate for the lack of spring precipitation, thereby ensuring a reliable supply of water for crop development in the long term. However, this approach was unable to account for the non-linear effect of water shortages during specific phenological stages on crop yields. Irrigation was carried out using the Center pivot technique, and the monthly amount of water was distributed evenly over two to three irrigation events, spaced two weeks apart. The first two rounds of watering were conducted in January, following a principle that was empirically established by the farmers as optimal for maintaining the moisture content of Vertisol, while minimizing water losses due to frequent irrigation. The remaining fields at each site served to verify the measurements obtained from the intensively monitored fields. Groundwater served as the primary source of irrigation water in the wheat fields. While direct measurements are typically more accurate, transpiration and evapotranspiration are challenging to measure and must be derived from the Cropwat table).

In Table 3, the validation of irrigation measurements was conducted for 14 wheat fields (C1, C2, C3, . . . , C14) from January to May. The validation included a comparison of the weekly evolution of irrigation and observed actual ET, along with the amount of irrigation and rainfall for each of the 14 wheat fields. The validation fields exhibited a high level of coherence, indicating the effectiveness of the irrigation hours in mitigating crop water stress through supplementary irrigation. In April, the center pivot of C12, C13, and C14 with regular irrigation had higher vegetation density and yield, as evidenced by NDVI, whereas fields in other center pivots had lower density. Integrating remote sensing techniques and meteorological data can provide valuable insights into the performance of an ideal irrigation system, which can enhance crop productivity. The study results suggest that remote sensing and meteorological data integration can facilitate the identification of optimal irrigation schedules and strategies for specific crops and regions. By monitoring vegetation health using remote sensing techniques, farmers and irrigation managers can adjust irrigation schedules to match crop water requirements, thereby reducing water waste and improving crop productivity. More frequent irrigation may be necessary in hot and dry conditions, whereas irrigation may not be required for a certain period.

### 3.3. NDVI and NDMI Time Series of Wheat Crop

In the period from January to May 2021, some center-pivot fields were planted with a single crop type, while others had alternating crop types, resulting in variations in NDVI and NDMI time series behavior. To examine this variation, NDVI and NDMI were compared for the Wheat Crop. Specifically, NDVI and NDMI were identified from 143 fields where only Wheat Crop was planted throughout the study period. The fields, each with a diameter of approximately 800 m, were divided into 2500 pixels, and the mean value for each field was determined by averaging the NDVI and NDMI of these pixels. Crop statistics were derived from the NDVI and NDMI time series data for the wheat crop, including maximum (Max) and minimum (Min) values, amplitude variation (Amp), and standard deviation (Std), to establish differences in time series behavior (see Appendix B Tables A2 and A3). In March and April, NDVI and NDMI values fluctuated significantly more in irrigated lands than in non-irrigated lands, possibly due to the influence of ETo and temperature on vegetation growth. To assess the changes in vegetation, the changes in classes (1, 2, 3, and 4) for NDVI and Dense, Moderate, Sparse, and Open soil classes were calculated. The category with the greatest change relative to the other four was then identified as the dominant category.

To demonstrate changes over time, the relative dominance of each class category was computed for each period. The NDVI and NDMI indices revealed that the non-irrigated portions of the field experienced drought conditions in February, March, and April, as indicated by the low NDVI values. The severity and extent of the drought varied over time and space. The values for January to May displayed spatial and temporal variability across the region, which can be attributed to the prevailing temperature and humidity conditions. The fluctuation in NDVI values is influenced by weather-related parameters such as rainfall, temperature, and humidity levels. Temporal variations in climate, soil, and temperature cause changes in NDVI values.

### 3.4. Evolutions of Observed NDVI and NDMI

While Figures 7 and 8 focused on the relationship between NDMI-based soil moisture and NDVI-based vegetation health in Wheat Crop, we aim to assess the possibility of detecting irrigation events using Sentinel-2 data by analyzing their association with real-world data. As illustrated in Figure 8, the NDMI in the center pivot area that was irrigated was notably higher than that in the nearby bare soil area.

In the Center pivot field, soil moisture levels were high due to irrigation, while the other field showed significant variability in soil moisture levels before June 2021. The wheat crop was grown and harvested frequently from January to June 2021, with irrigation durations ranging from 12 to 96 h, as per farmer records. The field was planted

with maize from August 2020 to December 2020, and irrigation maintained high soil moisture levels during that period. After the maize was picked, irrigation stopped until January 2021. This led to a sharp drop in the amount of water in the soil. However, soil moisture increased in mid-February 2021 after an 18 mm precipitation event from 11–15 February, which was captured by the Meteorological Station and resulted in an increase in both NDVI and NDMI (Figure 8). High temperatures are believed to impact vegetation strength and cause plant stress. The mean NDMI values increased in all center pivot irrigated fields, consistent with the trend of NDVI variation (see Figures 7 and 8). Although a lack of precipitation is typically the primary cause of drought, elevated potential evapotranspiration is associated with temperature and relative humidity. The evidence presented indicates that soil moisture plays a limiting role in the actual evapotranspiration process, especially during drought conditions, as it prevents excessive drying. Temperature and other factors that influence vegetation development and phenology also have an impact on actual evapotranspiration [48]. Thus, NDVI is a reliable sign of drought, and it is important to use empirical NDVI-NDMI-based indices to improve the performance of irrigation systems and increase crop yields. The average NDVI, which reflects the greenness of vegetation, is strongly linked to seasonal rainfall, indicating the potential use of NDVI as a drought predictor.

### 3.5. Correlation Matrix between NDVI and NDMI

Figure 9 displays the average NDVI time series profile for 2021, which shows a significant correlation between NDVI and NDMI. The projected green cover increased from about 0.40 to 0.80 between February and April, likely due to irrigation, before dropping to 0.6 by the end of April as irrigation decreased in preparation for the harvest season. The average NDVI increased due to an increase in NDMI but then dropped to 0.20 in May after the maturation and harvesting phase. Sentinel2 was able to detect changes in vegetation or physiological density accurately. All monthly index values were significantly correlated with meteorological parameters from various locations with a 95% confidence level. NDVI increased at several locations in the 143 center pivot and rain-fed area due to increased rainfall, irrigation, and temperature. The combination of moisture content and temperature played a significant role in reducing NDVI values. Ongoing land and crop degradation and yield losses occurred due to a lack of vegetation cover and relative humidity caused by insufficient rainfall during the growing season (Table A1). Increased temperatures can have severe natural consequences, increasing  $E_{To}$  and  $E_{Tc}$ . This suggests that crop development was not uniformly distributed across the region, even in times of water shortage, and some farmers were able to achieve acceptable crop growth by effectively using water through supplementary irrigation and implementing good agricultural practices. Remote-sensing-based NDVI and NDMI can provide valuable insights into the spatial and temporal distribution of crop irrigation water requirements at the field level, which can be compared to in situ monitoring of observed irrigation water supplied at the irrigation district scale. Acceptable estimates of  $E_{T0}$  and  $E_{Tc}$  for wheat (73.7, 98.4, 125.1, 229.4, and 319.2 mm/month) and (42.7, 57.1, 93.8, 229.4, and 383.0 mm/month) were obtained under various weather and water management conditions with irrigation periods of 12, 24, 48, 72, and 96 h, respectively, according to farmer records for the months from January to May. Figure 9 provide further details on this.

The significant rise in temperature can be attributed to the absence of rainfall, which caused a lack of moisture and resulted in higher  $E_{To}$  and  $E_{Tc}$ . One of the consequences of the increased  $E_{Tc}$  in April and May in the study area is the elevated temperature and decreased NDVI (Figure 9). This indicates the adverse effect of high temperature on the vegetation growth environment, resulting in lower vegetation values and area (NDVI) in the region. Only a few Center pivot areas in the study saw an increase in NDMI values, which was reflected in a vegetation increase in NDVI. Due to its location, Iraq's climate has transformed into a semi-arid climate, with a heavy influence from the Mediterranean climate characterized by hot, dry summers and warm, wet winters. Rainfall, temperature,

sunshine, and wind speed have a negative impact on wheat yield and chlorophyll content in semi-arid environments. The study suggests that the irrigation schedule followed by farmers compensated for the insufficient spring rainfall, resulting in sustainable crop growth. However, this approach did not consider the non-linear effects of water scarcity during specific phenological stages on crop yield. The newly proposed approach helps prevent harmful stress on wheat and ensures the proper distribution of water based on agronomic principles in a center pivot system. These results align with the findings of Polinova et al. (2019) [25].

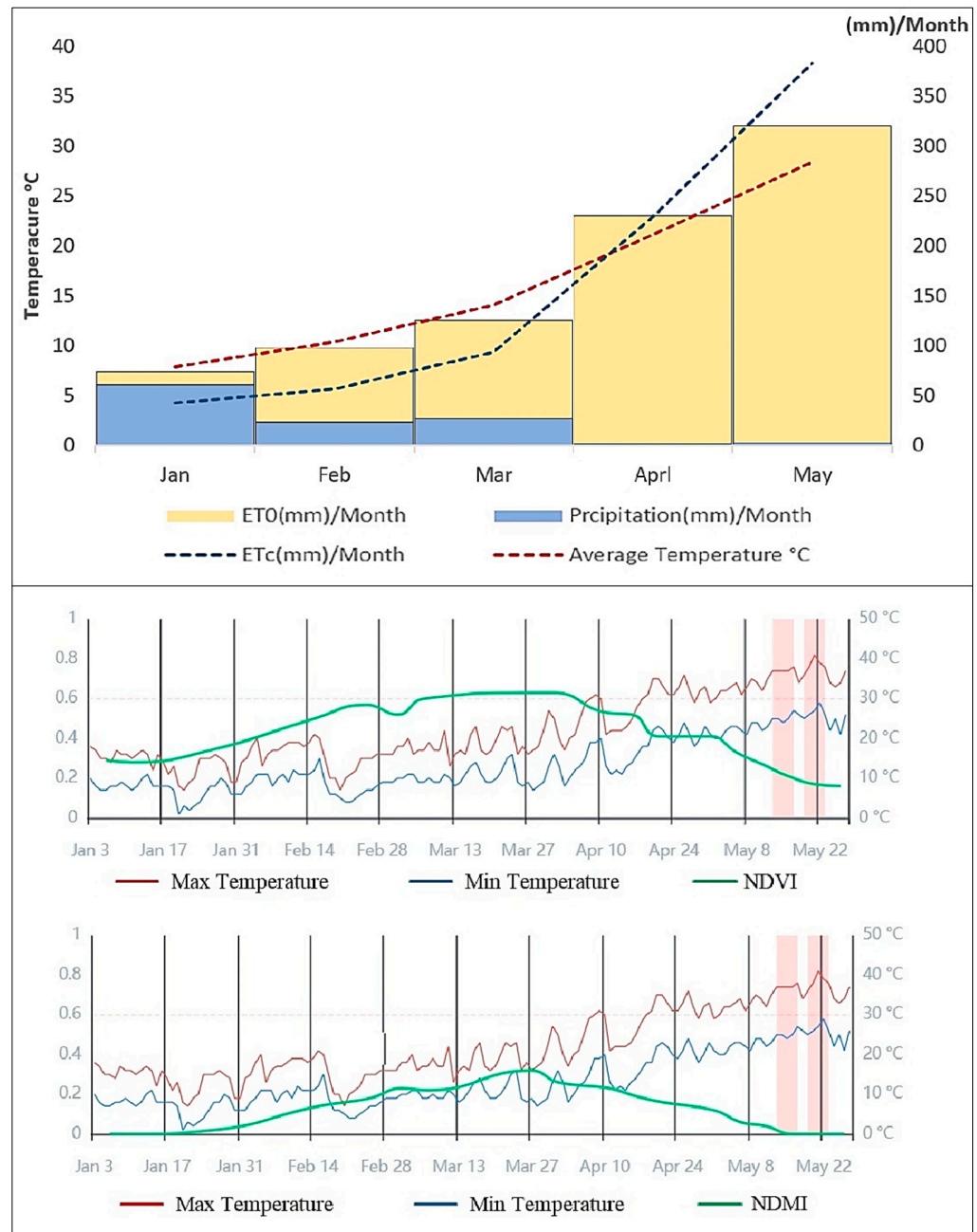


**Figure 9.** Monthly Precipitation, ETo, ETc, NDVI, NDMI, Average Temperature in study area recorded in 2021.

The NDVI has been associated with numerous vegetative properties, including photosynthetic capacity. Sufficient irrigation must be provided for a larger wheat yield to encourage strong output intensity. Figures 7 and 8 demonstrate the observed irrigation

water supply distribution, showcasing clear shifts from one month to another in both the applied and required irrigation water. The different shapes of the irrigation distribution reveal that farmers' use of irrigation water varies significantly from month to month, which may be influenced by both farmers' irrigation decision making and the small portion of crop water requirements met by rainfall, which was higher in the dry months of January and February 2021. During the research period (March), there was a slight increase in the average NDVI, although the increase was more noticeable. The average NDVI remained steady throughout the growing seasons (March to April). Even though 90% of the precipitation occurred during the growing seasons, annual precipitation varied greatly from 60.8 mm in January to 2.6 mm in May 2021 (Figures 9 and 10). These significant changes seemed to impact crop development, suggesting that sufficient irrigation water was available to support wheat growth throughout the growing season. This study defines water consumption as the amount of water that evaporates and seeps from an agricultural zone rather than the amount used for crop irrigation or diverted for that purpose. It was shown that by combining remote sensing and GIS techniques, a comprehensive evaluation of irrigation efficiency can be achieved for different irrigation systems [49].

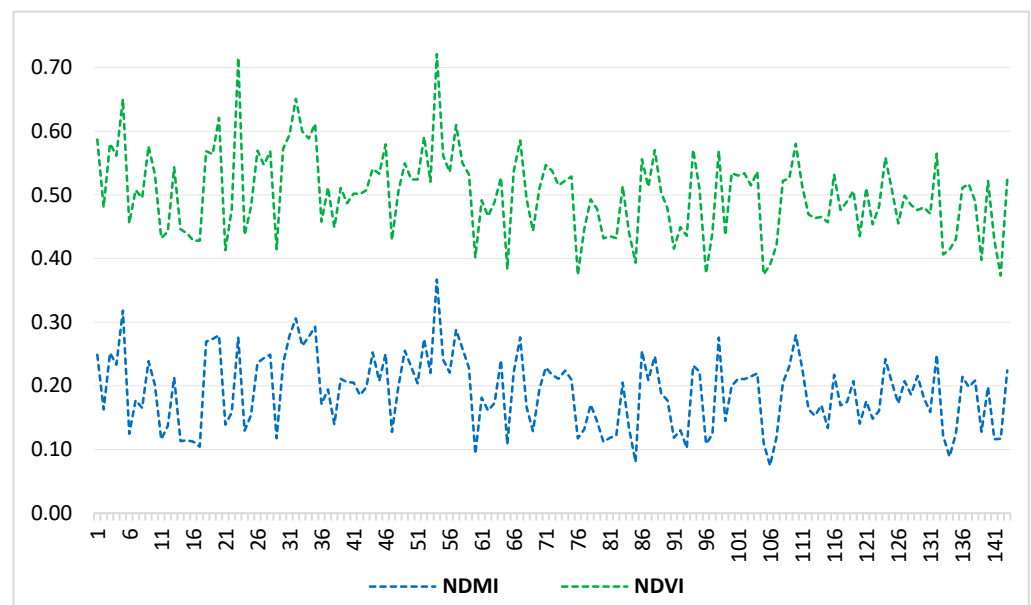
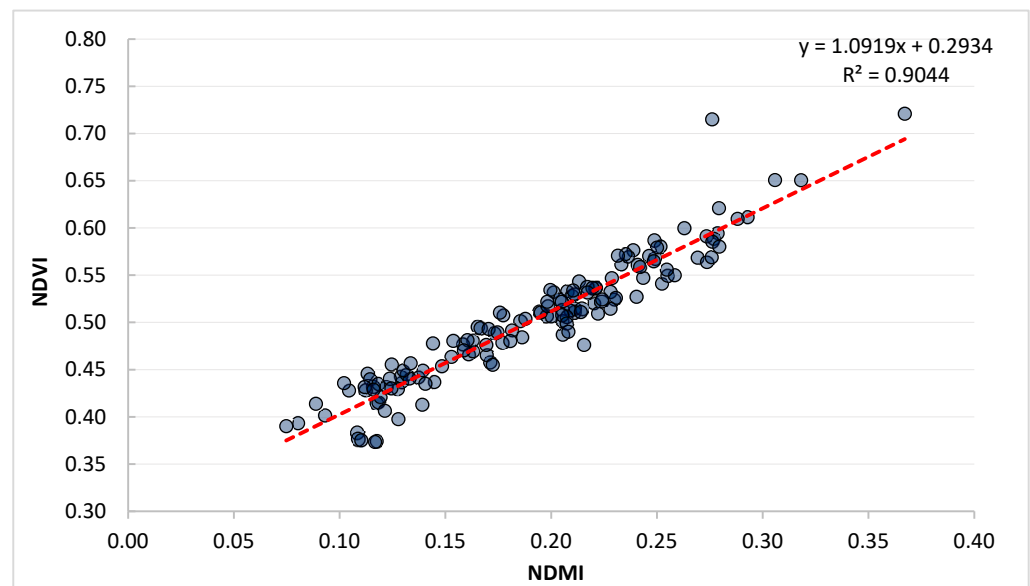


**Figure 10.** Temporal Variation of the NDVI and NDMI Value Based Vegetation Density Classes of 143 Center pivot wheat Field in 2021.

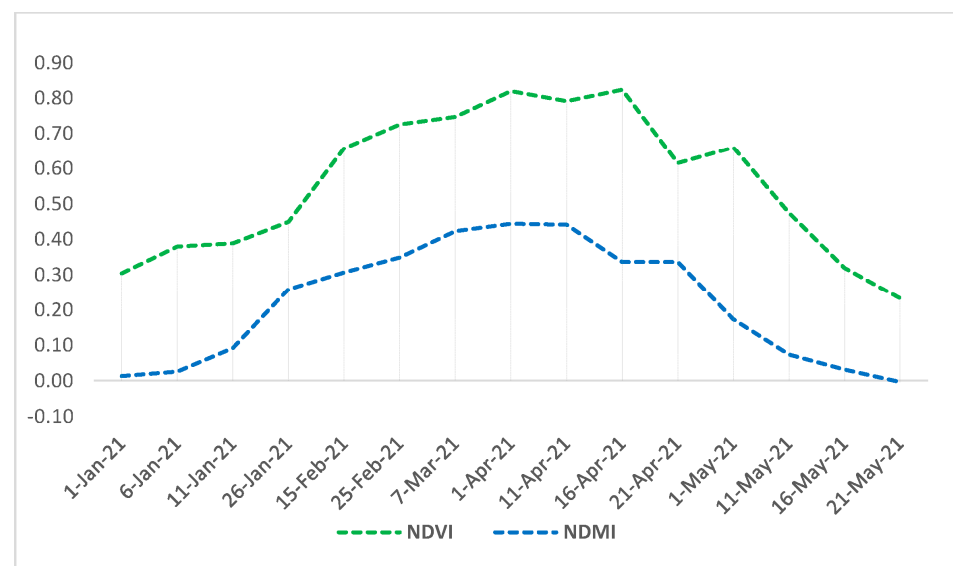
### 3.6. Crop Growing Period (NDVI)

Figure 11 displays the vegetation cover trend over a period of five months, indicating an upward trend in January, reaching its highest point in March and April, and declining to the lowest level at the end of May, which is consistent with the reported rates. The fluctuations in NDVI values during these months are heavily influenced by the precipitation and irrigation water requirements, as evidenced by the strong correlation between NDVI and NDMI, which varied in unison with an  $R^2$  of 0.904 (Figure 11). Remote sensing provides a holistic perspective of ground conditions. This study utilized available data to explore the correlation between irrigation schedules, crop yield, and remote sensing data. The final stage of the research involved a comparison of the findings obtained through the analysis of remote sensing data. By considering all the environmental factors that impact crop growth, and by evaluating the performance of irrigation, the study aimed to determine the root causes of variations in NDVI and NDMI values [50]. Nonetheless, it is worth mentioning that certain factors may not be pertinent or suitable in all situations [51,52]. The study period covered five months from January to May, with one growing season per year for wheat (Figure 4). The variability of climatic influences on drought, temporal changes, and

their relationship with precipitation, irrigation hours, ETo, ETc, and temperature is evident (Figure 12).



**Figure 11.** NDMI Correlation with NDVI-wheat in 143 Center pivot wheat Field -2021.



**Figure 12.** Temporal variation of the NDVI and NDMI value-based vegetation density classes of Center pivot wheat field from 1 January to 21 May 2021.

The NDVI is influenced by ETo, soil temperature, and irrigation, resulting in correlation values of 0.49, 0.55, and 0.76, respectively. Despite this, the growth rate of the crop is significantly affected by the NDMI. Although there is a strong relationship between NDMI and irrigation, with a correlation of approximately 0.91, it is not statistically significant, as shown in Figure 11 and Table A1. By analyzing 143 selected fields, it was found that the correlation between NDVI and NDMI increased the yield output when sufficient irrigation was provided in February, March, and April (Figure 11). Using EXLSTAT, the correlation coefficients for NDVI, NDMI, Irrigation, ETo, and ETc were calculated during the growing season spanning from January to May, an average of five months. These correlation coefficients are illustrated in Figures 12–14.

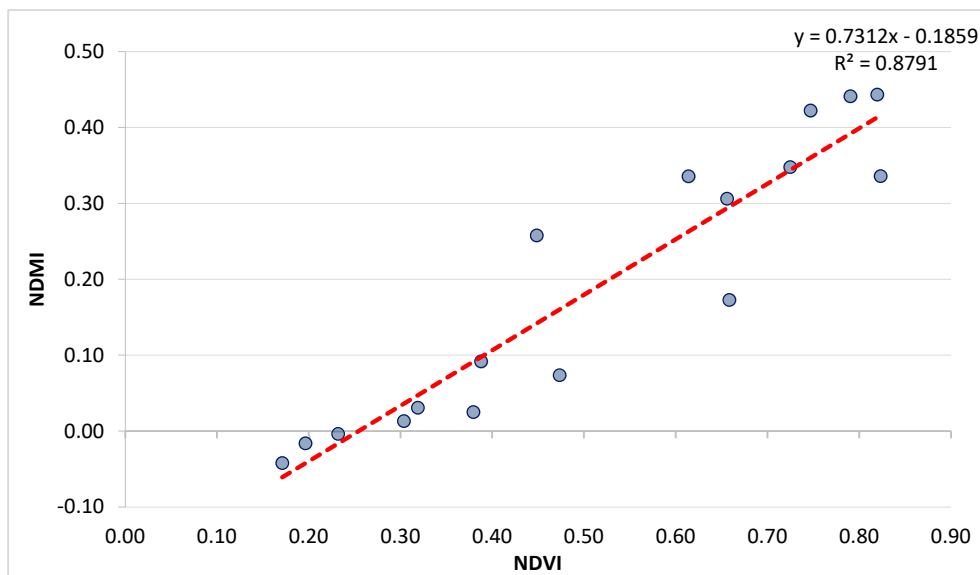


**Figure 13.** NDMI Correlation with NDVI-wheat in 143 Center pivot wheat field products with a 5-day temporal resolution.

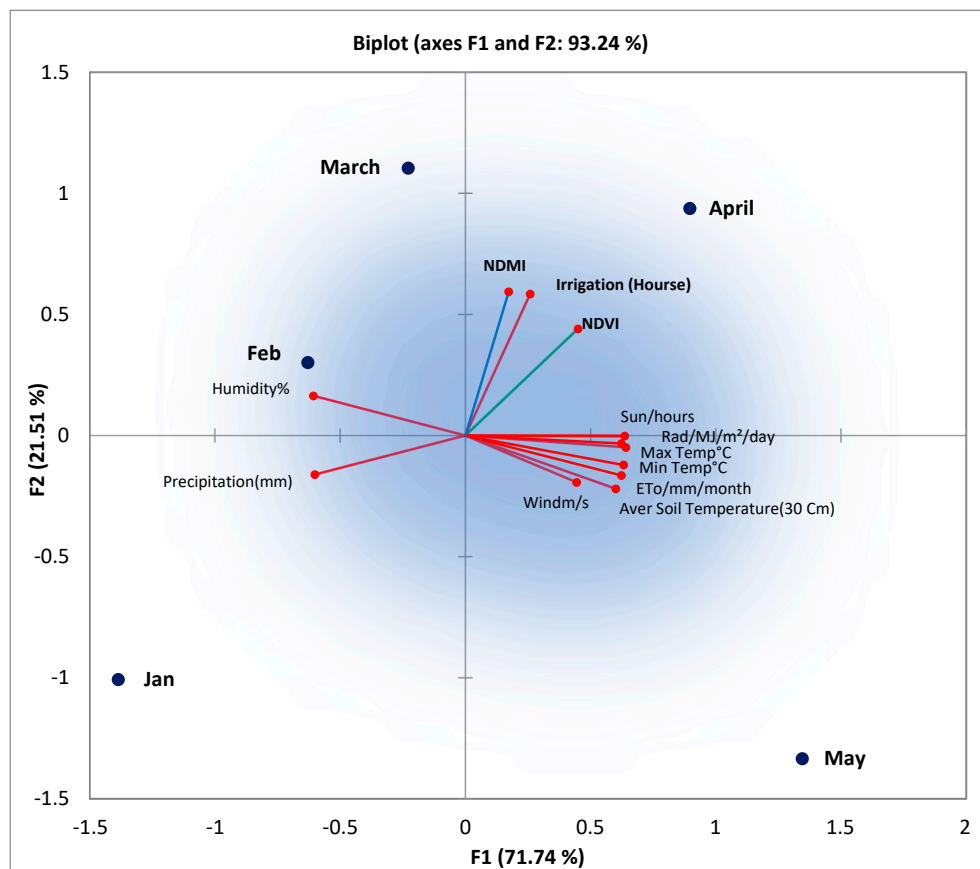


**Figure 14.** Principal Component Analysis of temporal Pattern changes of NDVI and NDMI with Meteorological parameters.

The findings revealed a strong and positive association between ETC and both NDVI and NDMI. Similarly, there was a positive correlation observed between NDVI and NDMI. These correlations between remote sensing-derived spectral indices and meteorological parameters were statistically significant. After 2020, the planting of maize ceased in the field, and the surface was bare until September 2021. Both time series of NDVI and NDMI present

fluctuations in vegetation, with peaks up to 1 and 0.5 for NDVI and NDMI, respectively, occurring during growing seasons. High values with a maximum NDVI of 1 and NDMI of 0.5 were observed in March 2021, which may have been caused by the presence of supplementary irrigation. The study also noticed through the trend of increasing the value of NDVI that the effect of supplementary irrigation during the months of the study was different, and this change mainly depended on the amount of precipitation falling for each month in the study area, and other environmental factors that also play a prominent role in the growth of the wheat crop (Figure 12). The results are consistent with multiple investigations [53–55].

Temperature is a key factor affecting the transpiration process of crops, as demonstrated by the significant fluctuation in ET<sub>0</sub> values between January and May, corresponding to the growth and harvest stages of the crop (Figure 13). Additionally, the wheat fields studied through farmer interviews were located in 14 Center pivot fields.

The fields had similar irrigation schedules, with an average of 48 irrigation hours distributed over two periods in January due to sufficient rainfall. However, in February, with a decrease in the precipitation rate and the application of fertilizers, the irrigation requirements of the fields increased to one hour, resulting in the need for three irrigation periods. PCA was utilized to determine the primary modes of variability in a dataset that examined the temporal changes in NDVI and NDMI in relation to meteorological parameters. NDVI and NDMI are remote sensing indices that are commonly used to monitor vegetation and moisture content, respectively (Figure 14). By examining the changes in these indices over time and their connection to temperature and precipitation, PCA identified the crucial factors influencing the changes in vegetation and moisture patterns. To carry out the PCA analysis, a covariance matrix of the dataset was constructed, and the matrix was eigendecomposed to obtain the principal components, which are linear combinations of the original variables that represent unique patterns of variability in the data. Typically, the first few principal components account for most of the variance in the dataset and are used to summarize the dominant modes of variability. The PCA of the temporal pattern changes in NDVI and NDMI in relation to meteorological parameters yielded valuable insights into the underlying factors responsible for changes in vegetation and moisture patterns over time and can aid in the identification of critical variables for monitoring and predicting these changes.

#### 4. Conclusions

The NDMI is a valuable tool for detecting moisture deficiencies in crops and identifying under-irrigated areas. This information can be used to divide fields into zones with different water needs and schedule precision irrigation events as needed. Crop Monitoring provides historical and current precipitation data, NDVI index graphs, and precipitation monitoring graphs. By analyzing seasonal weather and precipitation patterns, it is possible to plan precision irrigation strategies for different fields. In addition, Crop Monitoring offers a 5-day weather forecast for each field, which helps farmers decide on the need for watering activities to ensure proper soil moisture for crops. Precision irrigation is cost effective, providing sufficient water supply to crops in areas with limited rainfall. Crop Monitoring tracks changes in the NDVI for individual fields throughout the season. This helps farmers identify areas of weak and strong productivity across the field and create special maps for variable-rate applications of seeds and fertilizers. NDVI values can vary throughout the growing season, indicating water stress or waterlogging, and can be visualized through maps and graphs. Crop Monitoring also provides current and historical soil moisture data and NDVI index graphs, which help farmers track the correlation between rainfall and moisture levels in the field. NDMI values also vary throughout the growing season and can be visualized through maps and graphs, indicating water stress or waterlogging. A decrease in NDMI values suggests water stress, while abnormally high values could signal waterlogging. Visualization of NDMI through maps and graphs helps farmers detect problem areas in the field and save time and resources. Water supply is a critical

factor for plant growth, along with sunlight, nutrients, and soil temperature. While fields in areas with frequent rainfall receive sufficient water for crop growth, additional watering is necessary to maximize yields in semi-arid regions [56–58].

For a crop to progress from germination to the reproductive growth stage, where it can begin to produce grain, it requires at least 100 mm of water. It is worth mentioning that, according to the local meteorological station data, the 2021 crop season had the least precipitation and was classified as a drought season. In this study, the focus was on quantifying the loss of water due to evaporation from soil and transpiration from plants, which is collectively known as evapotranspiration. The most commonly used method for calculating evapotranspiration is to determine the reference evapotranspiration ( $E_{To}$ ), which is the amount of water that would be lost from a standardized grass surface under specific conditions [59].

The Penman–Monteith equation is often used to calculate  $E_{To}$ , taking into account weather variables such as temperature, humidity, wind speed, and solar radiation. To adjust  $E_{To}$  for different crop types, a crop coefficient ( $K_c$ ) is used, which represents the ratio of the actual evapotranspiration of a crop to the reference evapotranspiration. The  $K_c$  value is dependent on the crop growth stage, canopy cover, and other factors, and can be determined from tables or estimated using empirical formulas. Crop evapotranspiration ( $E_{Tc}$ ) is calculated by multiplying  $E_{To}$  with  $K_c$ , and it represents the amount of water required to meet the crop's water needs.  $E_{Tc}$  is calculated for each crop growth stage and added up over the entire growing season to estimate irrigation water requirements, which is the amount of water needed to supplement natural precipitation to meet the crop's water requirements. Irrigation water requirements can be calculated for different time periods, such as monthly, depending on the capacity of the irrigation system. This study engaged in collaboration with farmers and implemented a systematic approach to determine optimal irrigation water quantity and timing, aiming to satisfy crop water requirements, improve yield, reduce water usage, and address environmental concerns. The outcomes of this research align with findings from prior investigations. Furthermore, it was observed that the elevated temperatures in the growing season and spring led to heightened evaporation rates, necessitating longer irrigation periods [56–59].

This suggests a considerable need for additional irrigation during the drought year 2021. This study investigated the use of remote sensing techniques and meteorological data to assess the ideal irrigation system performance scenarios for improving crop productivity in the Erbil province of Iraq. The study period covered five months of the wheat growing season. The results demonstrated that vegetation coverage was significantly affected by climatic factors such as precipitation, irrigation hours, and temperature, particularly in the months of March, April, and May. The study also showed that the use of supplementary irrigation in rain-fed areas is essential to mitigate the impact of drought. The correlation between NDMI and NDVI was significant, likely due to the delayed effect of insufficient precipitation on vegetation. The Sentinel2 satellite provided accurate predictions of irrigation conditions, and the developed model was suitable for different time scales, ensuring the reliability and efficiency of water requirement predictions. Severe water stress was observed throughout the rain-fed area in March, April, and May, despite the widespread drought conditions in Iraq during that year. However, north Erbil's center pivot irrigation areas were unaffected by the lack of precipitation and water stress [56,57,60].

This study employed meteorological data and remote sensing-based indices to identify optimal irrigation schedules and water use anomalies. Including agricultural production and surface evaporation data could further improve the assessment of these factors during drought periods. Integrating remote sensing and evapotranspiration models can support irrigation managers in optimizing irrigation schedules and detecting areas with irrigation problems, leading to more efficient and sustainable irrigation practices. However, remote sensing techniques have limitations, such as inadequate spatial and temporal resolutions and inaccurate calibration. While continuous monitoring of the same field over multiple years is impractical due to the study area's crop rotation method, precision irrigation

systems that depend on integrated remote sensing and meteorological data can significantly impact agriculture and water resource management. Such systems can provide up-to-date information on crop health and moisture levels, which can be used to design and optimize precision irrigation systems that deliver water and nutrients where and when needed [56–58,60]. This approach can increase crop yields and quality, reduce water usage, and mitigate adverse environmental impacts such as soil erosion, nutrient leaching, and water runoff. Adopting precision irrigation systems based on remote sensing can also help address water scarcity issues at both the global and local levels, given that agriculture accounts for most freshwater usage worldwide. The development and adoption of such systems represent a significant advancement in agriculture and water resource management, which has the potential to enhance food security and environmental sustainability. Despite some moderate research linking wheat crops with NDMI and NDVI, there is still little investigation of wheat crop monitoring based on these indices in the KRI.

**Author Contributions:** Conceptualization, A.M.F.A.-Q., H.A.A.G. and K.M.; Data curation, H.A.A.G., A.M.F.A.-Q., H.A.S.R., K.K.H. and S.H.Z.; Formal analysis, H.A.A.G. and A.M.F.A.-Q.; Investigation, A.M.F.A.-Q., K.M., M.R. and H.A.A.G.; Methodology, H.A.A.G., K.K.H. and A.M.F.A.-Q.; Resources, A.M.F.A.-Q., K.M., H.A.S.R., S.H.Z. and H.A.A.G.; Supervision, A.M.F.A.-Q.; Validation, H.A.A.G. and A.M.F.A.-Q.; Visualization, A.M.F.A.-Q., P.H.A., M.R., K.K.H. and H.A.A.G.; Writing—original draft, A.M.F.A.-Q. and H.A.A.G.; Review, editing, improving, A.M.F.A.-Q., K.K.H., M.R., P.H.A. and K.K.H. All authors have read and agreed to the published version of the manuscript.

**Funding:** This research received no external funding.

**Data Availability Statement:** Some data in this manuscript were obtained from the Ministry of Agriculture and Water Resources, Kurdistan Region, Iraq, and the other data from the United States Geological Service (USGS) which provided the Landsat images freely on its website, and Statistical analysis of the parameters.

**Acknowledgments:** The authors extend their appreciation to the United States Geological Service (USGS) for making the Landsat images available on their website at no cost. Additionally, we express our deep gratitude to Ayad M. Fadhil Al-Quraishi of Tishk International University, Erbil, for funding the publication of this paper. We also want to thank Salahaddin University and Tishk International University in Erbil, Kurdistan Region, Iraq, for their valuable support. We are also thankful to Nuffic, the Orange Knowledge Programme, through the OKP-IRA-104278, Wageningen University & Research, The Netherlands, the Ministry of Agriculture and Water Resources/Water Resources Department.

**Conflicts of Interest:** The authors declare no conflict of interest.

## Appendix A

**Table A1.** Correlation matrix (Pearson (n)).

Variables	NDVI	NDMI	Precipitation (mm)	Min Temp °C	Max Temp °C	Humidity %	ETo/mm/Month	ETc/mm/Month	Soil Temperature (30 cm)	Irrigation (Hours)
NDVI	1.00	0.93	−0.86	0.42	0.63	−0.44	0.49	0.80	0.55	0.67
NDMI	0.93	1.00	−0.62	0.07	0.32	−0.12	0.15	0.59	0.22	0.89
Precipitation (mm)	−0.86	−0.62	1.00	−0.77	−0.89	0.78	−0.83	−0.95	−0.85	−0.26
Min Temp °C	0.42	0.07	−0.77	1.00	0.96	−0.96	0.99	0.79	0.98	−0.27
Max Temp °C	0.63	0.32	−0.89	0.96	1.00	−0.97	0.98	0.93	0.99	0.01
Humidity %	−0.44	−0.12	0.78	−0.96	−0.97	1.00	−0.98	−0.87	−0.98	0.14
ET0/mm/month	0.49	0.15	−0.83	0.99	0.98	−0.98	1.00	0.86	1.00	−0.17
ETc/mm/month	0.80	0.59	−0.95	0.79	0.93	−0.87	0.86	1.00	0.89	0.32
Soil Temperature	0.55	0.22	−0.85	0.98	0.99	−0.98	1.00	0.89	1.00	−0.11
Irrigation (h)	0.67	0.89	−0.26	−0.27	0.01	0.14	−0.17	0.32	−0.11	1.00

Note: Values in bold are different from 0 with a significance level  $\alpha = 0.05$ .

## Appendix B

Table A2. Monthly Average NDVI in 143 Center Pivot Values Zonal Statistics.

Field	NDVI-Jan	NDVI-Febf	NDVI-Mar	NDVI-Apr	NDVI-May	Count	Sum	Mean	St. Dev	Variance	Mean
1	0.71	0.81	0.81	0.77	0.31	2634.0	2209.8	0.84	0.07	0.00	0.84
2	0.20	0.56	0.72	0.83	0.53	2568.0	2198.4	0.86	0.04	0.00	0.86
3	0.65	0.85	0.84	0.80	0.31	1639.0	1425.4	0.87	0.05	0.00	0.87
4	0.57	0.85	0.83	0.80	0.35	1944.0	1678.4	0.86	0.04	0.00	0.86
5	0.84	0.88	0.85	0.80	0.36	2876.0	2507.8	0.87	0.04	0.00	0.87
6	0.18	0.43	0.61	0.80	0.53	3793.0	3089.1	0.81	0.08	0.01	0.81
7	0.41	0.61	0.68	0.79	0.44	1512.0	1237.9	0.82	0.03	0.00	0.82
8	0.40	0.61	0.62	0.76	0.43	864.0	693.0	0.80	0.06	0.00	0.80
9	0.57	0.76	0.81	0.83	0.42	865.0	765.2	0.88	0.04	0.00	0.88
10	0.40	0.70	0.77	0.80	0.47	1720.0	1417.8	0.82	0.06	0.00	0.82
11	0.19	0.53	0.65	0.73	0.45	835.0	632.5	0.76	0.06	0.00	0.76
12	0.25	0.54	0.69	0.79	0.38	1787.0	1479.5	0.83	0.07	0.00	0.83
13	0.42	0.76	0.81	0.81	0.46	1506.0	1269.7	0.84	0.04	0.00	0.84
14	0.21	0.25	0.37	0.72	0.66	1861.0	1229.1	0.66	0.18	0.03	0.66
15	0.25	0.62	0.67	0.65	0.44	829.0	558.1	0.67	0.12	0.01	0.67
16	0.23	0.56	0.65	0.74	0.38	1727.0	1332.9	0.77	0.06	0.00	0.77
17	0.18	0.43	0.62	0.74	0.47	1703.0	1363.0	0.80	0.06	0.00	0.80
18	0.40	0.78	0.79	0.84	0.58	2014.0	1732.6	0.86	0.04	0.00	0.86
19	0.44	0.82	0.81	0.80	0.53	2076.0	1773.0	0.85	0.04	0.00	0.85
20	0.72	0.89	0.88	0.81	0.37	985.0	854.9	0.87	0.05	0.00	0.87
21	0.29	0.59	0.65	0.60	0.33	1988.0	1420.8	0.71	0.23	0.05	0.71
22	0.24	0.56	0.66	0.77	0.55	844.0	662.4	0.78	0.05	0.00	0.78
23	0.73	0.79	0.66	0.74	0.77	874.0	730.8	0.84	0.10	0.01	0.84
24	0.22	0.51	0.59	0.78	0.44	1810.0	1451.4	0.80	0.06	0.00	0.80
25	0.25	0.70	0.78	0.74	0.48	1838.0	1412.2	0.77	0.05	0.00	0.77
26	0.45	0.77	0.80	0.77	0.56	1997.0	1627.5	0.81	0.14	0.02	0.81
27	0.38	0.77	0.78	0.81	0.55	2117.0	1778.2	0.84	0.04	0.00	0.84
28	0.44	0.79	0.83	0.82	0.52	1510.0	1300.7	0.86	0.04	0.00	0.86
29	0.17	0.49	0.60	0.76	0.40	1014.0	808.1	0.80	0.09	0.01	0.80
30	0.55	0.78	0.80	0.82	0.43	1986.0	1690.8	0.85	0.06	0.00	0.85
31	0.52	0.81	0.86	0.79	0.54	2013.0	1720.3	0.85	0.03	0.00	0.85
32	0.69	0.87	0.88	0.82	0.53	1699.0	1448.5	0.85	0.04	0.00	0.85
33	0.50	0.80	0.85	0.80	0.58	1097.0	938.9	0.86	0.05	0.00	0.86
34	0.50	0.86	0.85	0.82	0.52	3061.0	2688.2	0.88	0.04	0.00	0.88
35	0.63	0.86	0.85	0.83	0.44	1897.0	1628.4	0.86	0.04	0.00	0.86
36	0.27	0.72	0.81	0.75	0.35	1943.0	1653.0	0.85	0.05	0.00	0.85
37	0.32	0.69	0.74	0.81	0.49	1807.0	1531.8	0.85	0.03	0.00	0.85
38	0.29	0.61	0.71	0.74	0.33	2107.0	1663.0	0.79	0.05	0.00	0.79
39	0.56	0.83	0.81	0.63	0.31	1910.0	1511.9	0.79	0.04	0.00	0.79
40	0.52	0.81	0.80	0.65	0.26	1606.0	1311.1	0.82	0.03	0.00	0.82
41	0.37	0.75	0.81	0.75	0.41	2374.0	2018.5	0.85	0.09	0.01	0.85
42	0.42	0.71	0.75	0.77	0.36	2020.0	1614.6	0.80	0.07	0.00	0.80
43	0.22	0.60	0.72	0.80	0.64	3040.0	2545.3	0.84	0.06	0.00	0.84
44	0.41	0.81	0.81	0.80	0.46	2252.0	1917.3	0.85	0.05	0.00	0.85
45	0.45	0.79	0.81	0.77	0.41	4415.0	3704.2	0.84	0.04	0.00	0.84
46	0.48	0.82	0.85	0.81	0.51	4122.0	3596.2	0.87	0.03	0.00	0.87
47	0.35	0.61	0.66	0.67	0.30	1145.0	893.7	0.78	0.06	0.00	0.78
48	0.47	0.74	0.79	0.74	0.34	1445.0	1168.7	0.81	0.10	0.01	0.81
49	0.52	0.83	0.83	0.82	0.33	1663.0	1469.9	0.88	0.03	0.00	0.88
50	0.33	0.73	0.77	0.77	0.55	1074.0	900.4	0.84	0.05	0.00	0.84
51	0.44	0.77	0.81	0.79	0.37	1924.0	1611.9	0.84	0.04	0.00	0.84
52	0.46	0.84	0.87	0.83	0.56	3039.0	2651.7	0.87	0.03	0.00	0.87
53	0.25	0.67	0.79	0.83	0.59	1864.0	1625.3	0.87	0.04	0.00	0.87
54	0.73	0.89	0.90	0.84	0.69	1139.0	997.6	0.88	0.02	0.00	0.88
55	0.51	0.78	0.83	0.78	0.44	1167.0	972.6	0.83	0.04	0.00	0.83

Table A2. Cont.

Field	NDVI-Jan	NDVI-Febf	NDVI-Mar	NDVI-Apr	NDVI-May	Count	Sum	Mean	St. Dev	Variance	Mean
56	0.43	0.78	0.81	0.77	0.46	612.0	508.9	0.83	0.04	0.00	0.83
57	0.53	0.86	0.89	0.84	0.52	2074.0	1802.1	0.87	0.02	0.00	0.87
58	0.44	0.83	0.86	0.78	0.46	2331.0	2037.8	0.87	0.05	0.00	0.87
59	0.44	0.80	0.83	0.79	0.40	2475.0	2078.2	0.84	0.04	0.00	0.84
60	0.20	0.46	0.59	0.76	0.35	2504.0	1993.8	0.80	0.08	0.01	0.80
61	0.41	0.72	0.75	0.77	0.33	1957.0	1614.6	0.83	0.04	0.00	0.83
62	0.33	0.66	0.77	0.77	0.33	3045.0	2469.6	0.81	0.06	0.00	0.81
63	0.24	0.70	0.72	0.81	0.46	1678.0	1405.9	0.84	0.07	0.00	0.84
64	0.47	0.82	0.84	0.77	0.34	1829.0	1515.3	0.83	0.08	0.01	0.83
65	0.25	0.43	0.53	0.59	0.39	3014.0	2110.2	0.70	0.11	0.01	0.70
66	0.61	0.79	0.81	0.71	0.28	2074.0	1670.3	0.81	0.13	0.02	0.81
67	0.45	0.86	0.88	0.81	0.53	2009.0	1781.4	0.89	0.04	0.00	0.89
68	0.23	0.68	0.75	0.81	0.50	2264.0	1911.2	0.84	0.04	0.00	0.84
69	0.18	0.39	0.62	0.81	0.51	1767.0	1487.3	0.84	0.10	0.01	0.84
70	0.29	0.72	0.75	0.83	0.50	1618.0	1383.9	0.86	0.08	0.01	0.86
71	0.42	0.83	0.84	0.81	0.44	1870.0	1594.9	0.85	0.06	0.00	0.85
72	0.37	0.75	0.79	0.83	0.50	1966.0	1695.6	0.86	0.07	0.00	0.86
73	0.53	0.83	0.84	0.74	0.25	1208.0	1004.4	0.83	0.04	0.00	0.83
74	0.54	0.86	0.85	0.75	0.25	1013.0	859.8	0.85	0.03	0.00	0.85
75	0.74	0.80	0.77	0.61	0.20	1938.0	1482.1	0.76	0.06	0.00	0.76
76	0.26	0.53	0.58	0.50	0.33	2413.0	1588.0	0.66	0.29	0.08	0.66
77	0.16	0.30	0.51	0.82	0.58	1046.0	850.2	0.81	0.05	0.00	0.81
78	0.40	0.74	0.77	0.78	0.32	1906.0	1594.4	0.84	0.08	0.01	0.84
79	0.41	0.62	0.63	0.72	0.38	1521.0	1114.7	0.73	0.07	0.01	0.73
80	0.18	0.49	0.71	0.72	0.46	1378.0	1023.4	0.74	0.15	0.02	0.74
81	0.30	0.63	0.63	0.66	0.38	1226.0	858.2	0.70	0.06	0.00	0.70
82	0.32	0.63	0.73	0.68	0.30	2679.0	2022.2	0.75	0.07	0.00	0.75
83	0.47	0.82	0.81	0.75	0.33	1704.0	1401.2	0.82	0.06	0.00	0.82
84	0.27	0.67	0.68	0.73	0.36	954.0	740.3	0.78	0.06	0.00	0.78
85	0.31	0.56	0.60	0.62	0.27	2026.0	1393.7	0.69	0.18	0.03	0.69
86	0.47	0.84	0.85	0.82	0.41	1806.0	1568.4	0.87	0.06	0.00	0.87
87	0.40	0.77	0.77	0.77	0.40	1482.0	1202.8	0.81	0.06	0.00	0.81
88	0.41	0.80	0.85	0.84	0.53	1929.0	1682.8	0.87	0.03	0.00	0.87
89	0.39	0.65	0.70	0.78	0.44	1354.0	1115.4	0.82	0.03	0.00	0.82
90	0.28	0.61	0.72	0.77	0.47	3457.0	2815.9	0.81	0.09	0.01	0.81
91	0.22	0.47	0.55	0.73	0.42	1128.0	865.4	0.77	0.06	0.00	0.77
92	0.19	0.48	0.62	0.78	0.51	1553.0	1253.3	0.81	0.11	0.01	0.81
93	0.18	0.39	0.55	0.76	0.54	1193.0	910.4	0.76	0.10	0.01	0.76
94	0.58	0.80	0.81	0.77	0.43	1696.0	1386.2	0.82	0.05	0.00	0.82
95	0.42	0.83	0.85	0.82	0.29	1732.0	1499.9	0.87	0.04	0.00	0.87
96	0.16	0.39	0.55	0.76	0.32	1258.0	998.8	0.79	0.09	0.01	0.79
97	0.19	0.55	0.73	0.74	0.45	1606.0	1306.9	0.81	0.07	0.01	0.81
98	0.47	0.84	0.87	0.81	0.47	1800.0	1531.6	0.85	0.04	0.00	0.85
99	0.21	0.56	0.64	0.75	0.43	1882.0	1486.4	0.79	0.12	0.01	0.79
100	0.35	0.71	0.76	0.79	0.55	1706.0	1401.2	0.82	0.03	0.00	0.82
101	0.41	0.75	0.78	0.82	0.41	1430.0	1233.9	0.86	0.04	0.00	0.86
102	0.51	0.81	0.81	0.80	0.31	1954.0	1654.8	0.85	0.04	0.00	0.85
103	0.42	0.79	0.84	0.83	0.33	1796.0	1571.3	0.87	0.03	0.00	0.87
104	0.37	0.76	0.80	0.83	0.48	1864.0	1587.3	0.85	0.06	0.00	0.85
105	0.26	0.56	0.61	0.69	0.19	1693.0	1216.8	0.72	0.08	0.01	0.72
106	0.23	0.40	0.50	0.73	0.34	1807.0	1346.3	0.75	0.09	0.01	0.75
107	0.27	0.58	0.62	0.73	0.33	2854.0	2193.8	0.77	0.12	0.01	0.77
108	0.23	0.64	0.69	0.81	0.67	1813.0	1480.6	0.82	0.06	0.00	0.82
109	0.39	0.71	0.79	0.73	0.52	1619.0	1358.1	0.84	0.04	0.00	0.84
110	0.56	0.84	0.84	0.73	0.48	1872.0	1557.7	0.83	0.09	0.01	0.83
111	0.33	0.73	0.83	0.77	0.49	2219.0	1893.3	0.85	0.04	0.00	0.85
112	0.38	0.69	0.78	0.63	0.40	1124.0	930.3	0.83	0.06	0.00	0.83

Table A2. Cont.

Field	NDVI-Jan	NDVI-Febf	NDVI-Mar	NDVI-Apr	NDVI-May	Count	Sum	Mean	St. Dev	Variance	Mean
113	0.43	0.77	0.79	0.68	0.25	1222.0	955.1	0.78	0.09	0.01	0.78
114	0.31	0.58	0.70	0.80	0.38	1625.0	1365.7	0.84	0.07	0.00	0.84
115	0.23	0.56	0.72	0.77	0.47	3150.0	2604.8	0.83	0.07	0.00	0.83
116	0.40	0.75	0.80	0.80	0.45	2733.0	2322.8	0.85	0.10	0.01	0.85
117	0.41	0.75	0.77	0.71	0.31	1380.0	1075.2	0.78	0.07	0.00	0.78
118	0.16	0.54	0.76	0.83	0.60	908.0	789.5	0.87	0.03	0.00	0.87
119	0.42	0.71	0.77	0.76	0.39	1422.0	1153.8	0.81	0.09	0.01	0.81
120	0.22	0.65	0.73	0.75	0.33	1188.0	978.2	0.82	0.04	0.00	0.82
121	0.27	0.71	0.73	0.79	0.55	551.0	453.8	0.82	0.05	0.00	0.82
122	0.31	0.64	0.73	0.76	0.32	1740.0	1416.5	0.81	0.05	0.00	0.81
123	0.34	0.53	0.55	0.74	0.53	936.0	726.9	0.78	0.05	0.00	0.78
124	0.43	0.79	0.84	0.80	0.50	2891.0	2422.4	0.84	0.11	0.01	0.84
125	0.42	0.74	0.80	0.77	0.36	445.0	372.6	0.84	0.06	0.00	0.84
126	0.32	0.73	0.80	0.68	0.34	2584.0	2171.8	0.84	0.03	0.00	0.84
127	0.42	0.77	0.81	0.76	0.33	761.0	649.7	0.85	0.03	0.00	0.85
128	0.39	0.75	0.79	0.75	0.32	875.0	700.9	0.80	0.04	0.00	0.80
129	0.36	0.79	0.68	0.74	0.34	1960.0	1659.0	0.85	0.09	0.01	0.85
130	0.43	0.74	0.80	0.74	0.28	2010.0	1754.8	0.87	0.03	0.00	0.87
131	0.30	0.73	0.78	0.75	0.37	805.0	651.1	0.81	0.15	0.02	0.81
132	0.50	0.80	0.85	0.74	0.49	1836.0	1583.5	0.86	0.05	0.00	0.86
133	0.26	0.52	0.64	0.69	0.32	922.0	701.8	0.76	0.08	0.01	0.76
134	0.19	0.51	0.66	0.70	0.40	1071.0	821.4	0.77	0.07	0.00	0.77
135	0.19	0.56	0.73	0.78	0.36	941.0	801.6	0.85	0.03	0.00	0.85
136	0.50	0.82	0.83	0.81	0.21	1294.0	1131.7	0.87	0.03	0.00	0.87
137	0.47	0.83	0.85	0.74	0.32	1419.0	1214.4	0.86	0.02	0.00	0.86
138	0.33	0.64	0.74	0.74	0.48	935.0	808.2	0.86	0.02	0.00	0.86
139	0.29	0.64	0.71	0.71	0.17	1201.0	958.4	0.80	0.16	0.02	0.80
140	0.50	0.75	0.78	0.75	0.35	1148.0	923.8	0.80	0.16	0.03	0.80
141	0.19	0.37	0.54	0.75	0.50	957.0	706.4	0.74	0.12	0.01	0.74
142	0.26	0.55	0.62	0.61	0.23	3077.0	2179.4	0.71	0.18	0.03	0.71
143	0.43	0.82	0.84	0.81	0.33	1062.0	946.9	0.89	0.02	0.00	0.89

Table A3. Monthly Average NDMI in 143 Center Pivot Values Zonal Statistics.

Field	NDMI-Jan	NDMI-Feb	NDMI-Mar	NDMI-April	NDMI-May	Count	Sum	Mean	St. Dev	Variance	Mean
1	0.27	0.36	0.41	0.44	0.08	658.0	181.6	0.28	0.06	0.00	0.46
2	-0.10	0.17	0.32	0.45	0.18	643.0	-69.3	-0.11	0.03	0.00	0.44
3	0.23	0.45	0.47	0.43	0.07	410.0	85.4	0.21	0.09	0.01	0.47
4	0.15	0.44	0.44	0.43	0.10	484.0	61.0	0.13	0.08	0.01	0.45
5	0.40	0.46	0.45	0.47	0.15	722.0	296.8	0.41	0.10	0.01	0.50
6	-0.12	0.06	0.21	0.41	0.14	961.0	-113.2	-0.12	0.03	0.00	0.40
7	0.04	0.19	0.28	0.42	0.14	380.0	19.1	0.05	0.06	0.00	0.42
8	0.03	0.20	0.23	0.38	0.12	213.0	5.0	0.02	0.07	0.00	0.37
9	0.14	0.33	0.41	0.47	0.16	218.0	28.8	0.13	0.07	0.00	0.49
10	0.02	0.28	0.36	0.44	0.17	427.0	8.4	0.02	0.06	0.00	0.43
11	-0.09	0.12	0.22	0.35	0.12	210.0	-20.5	-0.10	0.02	0.00	0.34
12	-0.07	0.15	0.30	0.43	0.10	447.0	-38.0	-0.08	0.04	0.00	0.43
13	0.04	0.33	0.40	0.44	0.17	375.0	9.0	0.02	0.05	0.00	0.44
14	-0.09	-0.05	0.02	0.34	0.24	465.0	-19.2	-0.04	0.08	0.01	0.27
15	-0.05	0.21	0.28	0.28	0.09	207.0	-13.3	-0.06	0.03	0.00	0.29
16	-0.08	0.16	0.24	0.36	0.08	430.0	-40.3	-0.09	0.03	0.00	0.36
17	-0.10	0.07	0.20	0.37	0.11	425.0	-44.3	-0.10	0.03	0.00	0.39
18	0.03	0.36	0.39	0.50	0.31	508.0	2.8	0.01	0.03	0.00	0.47

Table A3. Cont.

Field	NDMI-Jan	NDMI-Feb	NDMI-Mar	NDMI-April	NDMI-May	Count	Sum	Mean	St. Dev	Variance	Mean
19	0.06	0.41	0.42	0.48	0.29	516.0	12.1	0.02	0.03	0.00	0.48
20	0.27	0.48	0.48	0.45	0.12	245.0	64.6	0.26	0.10	0.01	0.48
21	−0.04	0.20	0.27	0.29	0.15	501.0	−24.2	−0.05	0.06	0.00	0.35
22	−0.07	0.16	0.26	0.40	0.21	216.0	−20.4	−0.09	0.04	0.00	0.37
23	0.27	0.34	0.22	0.35	0.29	219.0	63.2	0.29	0.09	0.01	0.41
24	−0.08	0.14	0.20	0.40	0.12	450.0	−33.5	−0.07	0.03	0.00	0.38
25	−0.06	0.28	0.38	0.37	0.13	457.0	−37.8	−0.08	0.04	0.00	0.38
26	0.07	0.36	0.41	0.42	0.22	498.0	27.4	0.06	0.07	0.01	0.44
27	0.02	0.35	0.38	0.47	0.26	530.0	−1.5	0.00	0.03	0.00	0.45
28	0.06	0.38	0.44	0.47	0.23	374.0	15.2	0.04	0.06	0.00	0.47
29	−0.11	0.11	0.22	0.38	0.11	254.0	−29.5	−0.12	0.03	0.00	0.37
30	0.14	0.38	0.41	0.45	0.13	495.0	63.9	0.13	0.10	0.01	0.45
31	0.12	0.39	0.47	0.47	0.26	504.0	54.9	0.11	0.07	0.00	0.48
32	0.24	0.45	0.50	0.47	0.24	423.0	99.4	0.24	0.06	0.00	0.46
33	0.09	0.37	0.46	0.45	0.27	280.0	21.6	0.08	0.06	0.00	0.47
34	0.10	0.43	0.46	0.49	0.25	768.0	56.0	0.07	0.04	0.00	0.48
35	0.20	0.46	0.48	0.50	0.19	474.0	86.9	0.18	0.07	0.01	0.50
36	−0.07	0.27	0.39	0.42	0.15	488.0	−38.5	−0.08	0.05	0.00	0.45
37	−0.02	0.28	0.35	0.45	0.17	450.0	−15.4	−0.03	0.08	0.01	0.46
38	−0.03	0.20	0.31	0.38	0.08	530.0	−22.5	−0.04	0.04	0.00	0.40
39	0.15	0.42	0.42	0.34	0.11	479.0	68.8	0.14	0.09	0.01	0.42
40	0.13	0.40	0.40	0.36	0.10	405.0	48.0	0.12	0.09	0.01	0.44
41	0.02	0.31	0.40	0.43	0.18	591.0	1.9	0.00	0.04	0.00	0.44
42	0.04	0.30	0.34	0.40	0.11	502.0	11.7	0.02	0.06	0.00	0.40
43	−0.09	0.19	0.31	0.45	0.30	763.0	−82.3	−0.11	0.03	0.00	0.42
44	0.05	0.38	0.41	0.47	0.23	564.0	9.5	0.02	0.04	0.00	0.47
45	0.06	0.38	0.43	0.43	0.11	1099.0	36.7	0.03	0.06	0.00	0.45
46	0.08	0.41	0.46	0.47	0.20	1036.0	62.0	0.06	0.06	0.00	0.49
47	−0.01	0.20	0.22	0.33	0.08	287.0	−3.4	−0.01	0.06	0.00	0.35
48	0.09	0.31	0.38	0.40	0.12	357.0	28.8	0.08	0.08	0.01	0.43
49	0.11	0.40	0.43	0.46	0.18	415.0	38.8	0.09	0.06	0.00	0.47
50	0.00	0.32	0.36	0.44	0.26	267.0	−7.0	−0.03	0.02	0.00	0.43
51	0.06	0.33	0.39	0.43	0.13	482.0	25.4	0.05	0.07	0.00	0.44
52	0.07	0.41	0.48	0.49	0.27	761.0	29.2	0.04	0.06	0.00	0.49
53	−0.07	0.24	0.37	0.49	0.30	464.0	−37.1	−0.08	0.05	0.00	0.46
54	0.28	0.48	0.54	0.52	0.35	284.0	80.6	0.28	0.09	0.01	0.53
55	0.11	0.35	0.43	0.46	0.18	292.0	28.9	0.10	0.08	0.01	0.48
56	0.05	0.35	0.41	0.44	0.18	150.0	5.0	0.03	0.06	0.00	0.45
57	0.13	0.43	0.49	0.50	0.25	518.0	56.5	0.11	0.07	0.00	0.49
58	0.06	0.39	0.45	0.46	0.24	588.0	26.0	0.04	0.07	0.00	0.47
59	0.08	0.37	0.41	0.43	0.19	618.0	33.3	0.05	0.04	0.00	0.43
60	−0.10	0.09	0.18	0.36	0.05	627.0	−66.5	−0.11	0.02	0.00	0.38
61	0.04	0.32	0.36	0.41	0.08	486.0	4.2	0.01	0.04	0.00	0.43
62	−0.02	0.26	0.37	0.41	0.09	761.0	−17.2	−0.02	0.05	0.00	0.42
63	−0.09	0.28	0.31	0.43	0.18	421.0	−46.1	−0.11	0.03	0.00	0.41
64	0.11	0.40	0.46	0.44	0.17	458.0	53.2	0.12	0.04	0.00	0.45
65	−0.05	0.09	0.16	0.28	0.15	754.0	−40.9	−0.05	0.05	0.00	0.31
66	0.19	0.37	0.42	0.41	0.07	519.0	99.6	0.19	0.11	0.01	0.46
67	0.07	0.42	0.48	0.48	0.27	503.0	21.5	0.04	0.05	0.00	0.48
68	−0.09	0.25	0.33	0.43	0.16	566.0	−57.9	−0.10	0.05	0.00	0.43
69	−0.11	0.05	0.21	0.43	0.17	442.0	−51.1	−0.12	0.09	0.01	0.43
70	−0.04	0.30	0.35	0.46	0.20	407.0	−12.6	−0.03	0.07	0.01	0.45
71	0.05	0.42	0.48	0.45	0.15	466.0	11.1	0.02	0.04	0.00	0.46
72	0.00	0.33	0.39	0.47	0.21	491.0	−17.1	−0.03	0.04	0.00	0.46
73	0.13	0.39	0.42	0.40	0.09	306.0	39.1	0.13	0.06	0.00	0.44
74	0.13	0.42	0.45	0.42	0.10	253.0	32.3	0.13	0.06	0.00	0.47
75	0.31	0.37	0.36	0.29	0.04	487.0	156.2	0.32	0.12	0.02	0.39

Table A3. Cont.

Field	NDMI-Jan	NDMI-Feb	NDMI-Mar	NDMI-April	NDMI-May	Count	Sum	Mean	St. Dev	Variance	Mean
76	−0.05	0.15	0.22	0.24	0.16	605.0	−37.9	−0.06	0.05	0.00	0.30
77	−0.12	−0.01	0.14	0.44	0.19	256.0	−31.5	−0.12	0.03	0.00	0.41
78	0.02	0.30	0.36	0.41	0.07	476.0	9.3	0.02	0.05	0.00	0.43
79	0.04	0.22	0.23	0.33	0.08	378.0	17.1	0.05	0.08	0.01	0.32
80	−0.12	0.11	0.30	0.35	0.12	347.0	−46.1	−0.13	0.05	0.00	0.37
81	−0.02	0.21	0.23	0.29	0.09	307.0	−10.9	−0.04	0.04	0.00	0.30
82	−0.02	0.22	0.32	0.31	0.04	671.0	−19.3	−0.03	0.04	0.00	0.36
83	0.09	0.41	0.43	0.39	0.09	426.0	26.9	0.06	0.07	0.00	0.43
84	−0.04	0.27	0.29	0.35	0.06	239.0	−11.0	−0.05	0.03	0.00	0.36
85	−0.03	0.16	0.20	0.26	0.00	506.0	−17.7	−0.04	0.09	0.01	0.30
86	0.08	0.42	0.45	0.49	0.20	450.0	24.1	0.05	0.06	0.00	0.48
87	0.04	0.35	0.37	0.42	0.16	368.0	5.1	0.01	0.05	0.00	0.40
88	0.04	0.37	0.44	0.48	0.23	485.0	0.8	0.00	0.05	0.00	0.47
89	0.03	0.26	0.30	0.43	0.15	343.0	3.0	0.01	0.04	0.00	0.43
90	−0.04	0.22	0.32	0.43	0.18	863.0	−49.0	−0.06	0.06	0.00	0.42
91	−0.08	0.11	0.17	0.38	0.12	282.0	−28.0	−0.10	0.04	0.00	0.37
92	−0.10	0.11	0.22	0.41	0.14	387.0	−38.6	−0.10	0.04	0.00	0.40
93	−0.11	0.04	0.14	0.36	0.15	302.0	−32.1	−0.11	0.04	0.00	0.34
94	0.15	0.37	0.40	0.41	0.14	432.0	60.1	0.14	0.09	0.01	0.42
95	0.05	0.41	0.44	0.49	0.10	430.0	10.8	0.03	0.06	0.00	0.50
96	−0.11	0.06	0.16	0.37	0.15	316.0	−39.2	−0.12	0.05	0.00	0.36
97	−0.09	0.14	0.30	0.37	0.10	402.0	−36.6	−0.09	0.03	0.00	0.40
98	0.08	0.42	0.48	0.49	0.24	438.0	25.5	0.06	0.06	0.00	0.49
99	−0.08	0.17	0.24	0.39	0.14	469.0	−42.2	−0.09	0.05	0.00	0.39
100	−0.02	0.29	0.37	0.43	0.19	428.0	−11.7	−0.03	0.05	0.00	0.44
101	0.05	0.34	0.39	0.47	0.13	361.0	18.1	0.05	0.08	0.01	0.47
102	0.11	0.40	0.42	0.43	0.07	485.0	45.2	0.09	0.08	0.01	0.45
103	0.04	0.36	0.43	0.47	0.12	450.0	11.2	0.02	0.05	0.00	0.48
104	0.01	0.34	0.41	0.46	0.20	465.0	−1.8	0.00	0.06	0.00	0.44
105	−0.04	0.17	0.23	0.31	0.07	424.0	−22.3	−0.05	0.03	0.00	0.32
106	−0.09	0.05	0.12	0.34	0.04	453.0	−42.9	−0.09	0.04	0.00	0.32
107	−0.05	0.19	0.23	0.36	0.07	711.0	−49.6	−0.07	0.03	0.00	0.37
108	−0.07	0.22	0.30	0.44	0.30	453.0	−31.7	−0.07	0.03	0.00	0.42
109	0.04	0.29	0.38	0.42	0.27	405.0	9.5	0.02	0.07	0.00	0.44
110	0.16	0.42	0.45	0.43	0.27	467.0	70.1	0.15	0.07	0.01	0.45
111	0.02	0.31	0.42	0.45	0.25	554.0	−2.8	0.00	0.07	0.00	0.47
112	0.02	0.26	0.36	0.33	0.14	284.0	4.8	0.02	0.06	0.00	0.41
113	0.06	0.35	0.37	0.32	0.02	305.0	17.6	0.06	0.07	0.01	0.37
114	−0.02	0.19	0.30	0.45	0.14	407.0	−13.5	−0.03	0.05	0.00	0.45
115	−0.08	0.16	0.31	0.38	0.12	785.0	−67.0	−0.09	0.03	0.00	0.41
116	0.04	0.33	0.40	0.44	0.18	684.0	13.2	0.02	0.06	0.00	0.44
117	0.04	0.33	0.37	0.35	0.08	345.0	9.5	0.03	0.06	0.00	0.38
118	−0.14	0.14	0.34	0.48	0.25	228.0	−35.0	−0.15	0.02	0.00	0.46
119	0.07	0.30	0.36	0.41	0.16	353.0	20.7	0.06	0.05	0.00	0.42
120	−0.08	0.23	0.32	0.39	0.08	298.0	−26.5	−0.09	0.04	0.00	0.42
121	−0.04	0.28	0.33	0.43	0.15	138.0	−8.9	−0.06	0.02	0.00	0.43
122	−0.02	0.23	0.32	0.39	0.07	432.0	−14.7	−0.03	0.04	0.00	0.41
123	0.00	0.14	0.17	0.38	0.21	236.0	−2.4	−0.01	0.05	0.00	0.35
124	0.05	0.35	0.43	0.46	0.24	717.0	14.7	0.02	0.05	0.00	0.45
125	0.05	0.31	0.39	0.42	0.16	119.0	3.8	0.03	0.09	0.01	0.46
126	0.00	0.31	0.40	0.37	0.13	646.0	−10.5	−0.02	0.03	0.00	0.45
127	0.06	0.35	0.40	0.43	0.14	191.0	7.3	0.04	0.04	0.00	0.46
128	0.06	0.34	0.39	0.39	0.10	213.0	7.5	0.04	0.05	0.00	0.39
129	0.04	0.37	0.35	0.42	0.20	493.0	3.2	0.01	0.05	0.00	0.46
130	0.05	0.31	0.39	0.39	0.10	500.0	15.0	0.03	0.06	0.00	0.46
131	−0.05	0.32	0.40	0.39	0.08	199.0	−14.2	−0.07	0.05	0.00	0.41
132	0.08	0.35	0.46	0.43	0.25	458.0	35.8	0.08	0.13	0.02	0.47

Table A3. Cont.

Field	NDMI-Jan	NDMI-Feb	NDMI-Mar	NDMI-April	NDMI-May	Count	Sum	Mean	St. Dev	Variance	Mean
133	−0.05	0.14	0.25	0.35	0.09	230.0	−9.5	−0.04	0.04	0.00	0.36
134	−0.10	0.12	0.24	0.33	0.06	269.0	−26.7	−0.10	0.03	0.00	0.35
135	−0.10	0.15	0.29	0.41	0.08	236.0	−24.2	−0.10	0.02	0.00	0.44
136	0.08	0.39	0.42	0.44	0.10	324.0	16.6	0.05	0.08	0.01	0.47
137	0.09	0.39	0.45	0.42	0.06	354.0	20.4	0.06	0.05	0.00	0.48
138	0.00	0.24	0.36	0.42	0.25	233.0	−4.0	−0.02	0.04	0.00	0.48
139	−0.03	0.24	0.30	0.34	0.05	297.0	−9.8	−0.03	0.06	0.00	0.38
140	0.09	0.33	0.37	0.40	0.10	288.0	23.7	0.08	0.07	0.00	0.41
141	−0.10	0.04	0.16	0.38	0.15	240.0	−28.2	−0.12	0.07	0.00	0.34
142	−0.04	0.16	0.24	0.29	0.10	770.0	−36.6	−0.05	0.05	0.00	0.32
143	0.06	0.37	0.43	0.45	0.16	268.0	11.4	0.04	0.04	0.00	0.46

## References

- Ghazaryan, G.; König, S.; Rezaei, E.E.; Siebert, S.; Dubovyk, O. Analysis of Drought Impact on Croplands from Global to Regional Scale: A Remote Sensing Approach. *Remote Sens.* **2020**, *12*, 4030. [\[CrossRef\]](#)
- Ministry of Agriculture and Water Resources. *Review of the Agricultural Sector in the Kurdistan Region of Iraq: Analysis on Crops, Water Resources And Irrigation, and Selected Value Chains*; Annual Report; Ministry of Agriculture and Water Resources: Erbil, Iraq, 2019.
- Yousuf, M.A.; Rapantova, N.; Younis, J.H. Sustainable Water Management in Iraq (Kurdistan) as a Challenge for Governmental Responsibility. *Water* **2018**, *10*, 1651. [\[CrossRef\]](#)
- Dong, J.; Liu, W.; Han, W.; Xiang, K.; Lei, T.; Yuan, W. A Phenology-Based Method for Identifying the Planting Fraction of Winter Wheat Using Moderate-Resolution Satellite Data. *Int. J. Remote Sens.* **2020**, *41*, 6892–6913. [\[CrossRef\]](#)
- Jin, X.; Kumar, L.; Li, Z.; Xu, X.; Yang, G.; Wang, J. Estimation of Winter Wheat Biomass and Yield by Combining the Aquacrop Model and Field Hyperspectral Data. *Remote Sens.* **2016**, *8*, 972. [\[CrossRef\]](#)
- Van Dam, J.C.; Singh, R.; Bessembinder, J.J.E.; Leffelaar, P.A.; Bastiaanssen, W.G.M.; Jhorar, R.K.; Kroes, J.G.; Droogers, P. Assessing Options to Increase Water Productivity in Irrigated River Basins Using Remote Sensing and Modelling Tools. *Int. J. Water Resour. Dev.* **2006**, *22*, 115–133. [\[CrossRef\]](#)
- Kamal, K.; Hakzi, A. Spatiotemporal Variation of Wheat Yield and Water Productivity in Centre Pivot Irrigation Systems. Master's Thesis, IHE Delft Institute for Water Education, Delft, The Netherlands, 2022.
- FAO; WFP. *Dates, Grapes, Tomatoes and Wheat*; Food and Agriculture Organization: Rome, Italy, 2021; ISBN 9789251336342.
- Huang, J.; Sedano, F.; Huang, Y.; Ma, H.; Li, X.; Liang, S.; Tian, L.; Zhang, X.; Fan, J.; Wu, W. Assimilating a Synthetic Kalman Filter Leaf Area Index Series into the WOFOST Model to Improve Regional Winter Wheat Yield Estimation. *Agric. For. Meteorol.* **2016**, *216*, 188–202. [\[CrossRef\]](#)
- Morel, J.; Bégué, A.; Todoroff, P.; Martiné, J.-F.; Lebourgeois, V.; Petit, M. Coupling a Sugarcane Crop Model with the Remotely Sensed Time Series of FIPAR to Optimise the Yield Estimation. *Eur. J. Agron.* **2014**, *61*, 60–68. [\[CrossRef\]](#)
- FAO; IHE Delft. *Water Accounting in the Jordan River Basin, Remote Sensing for Water Productivity*; Food and Agriculture Organization: Rome, Italy, 2020; ISBN 9789251326619.
- Nichols, P.D.; Murphy, M.K.; Kenney, D.S. *Water and Growth in Colorado*; Natural Resources Law Center: Boulder, CO, USA, 2021; ISBN 1045021091.
- International Organization for Migration. *All Small Scale Irrigation Infrastructure Development in Iraq: A Feasibility Review*; International Organization for Migration: Grand-Saconnex, Switzerland, 2022.
- Schnepf, R. Iraq Agriculture and Food Supply: Background and Issues. *CRS Rep. Congr.* **2004**, *57*, 62.
- Bastiaanssen, W.G.M.; Molden, D.J.; Makin, I.W. Remote Sensing for Irrigated Agriculture: Examples from Research and Possible Applications. *Agric. Water Manag.* **2000**, *46*, 137–155. [\[CrossRef\]](#)
- FAO; IHE Delft. *WaPOR Quality Assessment*; Food and Agriculture Organization: Rome, Italy, 2019; ISBN 9789251315354.
- Jaradat, A. Agriculture in Iraq: Resources, Potentials, Constraints, Research Needs and Priorities. *Agriculture* **2003**, *1*, 160–166.
- Cooper, B.P.J.M.; Gregoryf, P.J.; Tully, D.; Harris, H.C.; August, A. Improving water use efficiency of annual crops in the rainfed farming systems of west asia and north africa. *Exp. Agric.* **1987**, *23*, 113–158. [\[CrossRef\]](#)
- Jin, X.; Yang, G.; Li, Z.; Xu, X.; Wang, J.; Lan, Y. Estimation of Water Productivity in Winter Wheat Using the AquaCrop Model with Field Hyperspectral Data. *Precis. Agric.* **2018**, *19*, 1–17. [\[CrossRef\]](#)
- Awchi, T.A.; Jasim, A.I. Rainfall Data Analysis and Study of Meteorological Draught in Iraq for the Period 1970–2010. *Tikrit J. Eng. Sci.* **2017**, *24*, 110–121. [\[CrossRef\]](#)
- Gaznayee, H.A.A.; Al-Quraishi, A.M.F.; Mahdi, K.; Ritsema, C. A Geospatial Approach for Analysis of Drought Impacts on Vegetation Cover and Land Surface Temperature in the Kurdistan Region of Iraq. *Water* **2022**, *14*, 927. [\[CrossRef\]](#)

22. Al-Quraishi, A.M.F.; Gaznayee, H.A.; Crespi, M. Drought Trend Analysis in a Semi-Arid Area of Iraq Based on Normalized Difference Vegetation Index, Normalized Difference Water Index and Standardized Precipitation Index. *J. Arid Land* **2021**, *13*, 413–430. [[CrossRef](#)]
23. Namdar, R.; Karami, E.; Keshavarz, M. Climate Change and Vulnerability: The Case of Mena Countries. *ISPRS Int. J. Geo-Inf.* **2021**, *10*, 794. [[CrossRef](#)]
24. Ahmad, M.D.; Turrall, H.; Nazeer, A. Diagnosing Irrigation Performance and Water Productivity through Satellite Remote Sensing and Secondary Data in a Large Irrigation System of Pakistan. *Agric. Water Manag.* **2009**, *96*, 551–564. [[CrossRef](#)]
25. Polinova, M.; Salinas, K.; Bonfante, A.; Brook, A. Irrigation Optimization under a Limited Water Supply by the Integration of Modern Approaches into Traditional Water Management on the Cotton Fields. *Remote Sens.* **2019**, *11*, 2127. [[CrossRef](#)]
26. Mustafa, M.T.; Hassoon, K.I.; Hussain, H.M.; Modher, H. Using Water Indices (Ndwi, Mndwi, NDMI, WRI and AWEI) to Detect Physical and Chemical Parameters by Apply. *Int. J. Res.-Granthaalayah* **2017**, *5*, 117–128. [[CrossRef](#)]
27. Elbeltagi, A.; Aslam, M.R.; Mokhtar, A.; Deb, P.; Abubakar, G.A.; Kushwaha, N.L.; Venancio, L.P.; Malik, A.; Kumar, N.; Deng, J. Spatial and Temporal Variability Analysis of Green and Blue Evapotranspiration of Wheat in the Egyptian Nile Delta from 1997 to 2017. *J. Hydrol.* **2021**, *594*, 125662. [[CrossRef](#)]
28. Gaznayee, H.A.; Al-Quraishi, A.M.F. Analysis of Agricultural Drought's Severity and Impacts in Erbil Province, the Iraqi Kurdistan Region Based on Time Series NDVI and TCI Indices for 1998 through 2017. *J. Adv. Res. Dyn. Control Syst.* **2019**, *11*, 287–297. [[CrossRef](#)]
29. Wan, Z.; Wang, P. Using MODIS Land Surface Temperature and Normalized Difference Vegetation Index Products for Monitoring Drought in the Southern Great Plains, USA. *Int. J. Remote Sens.* **2004**, *25*, 61–72. [[CrossRef](#)]
30. Heydari, H.; Zoj, M.J.V.; Maghsoudi, Y.; Dehnavi, S. An Investigation of Drought Prediction Using Various Remote-Sensing Vegetation Indices for Different Time Spans. *Int. J. Remote Sens.* **2018**, *39*, 1871–1889. [[CrossRef](#)]
31. Qader, S.H.; Dash, J.; Atkinson, P.M. Forecasting Wheat and Barley Crop Production in Arid and Semi-Arid Regions Using Remotely Sensed Primary Productivity and Crop Phenology: A Case Study in Iraq. *Sci. Total Environ.* **2018**, *613–614*, 250–262. [[CrossRef](#)] [[PubMed](#)]
32. Jaafar, H.H.; Ahmad, F.A. Crop Yield Prediction from Remotely Sensed Vegetation Indices and Primary Productivity in Arid and Semi-Arid Lands. *Int. J. Remote Sens.* **2015**, *36*, 4570–4589. [[CrossRef](#)]
33. Bolton, D.K.; Friedl, M.A. Forecasting Crop Yield Using Remotely Sensed Vegetation Indices and Crop Phenology Metrics. *Agric. For. Meteorol.* **2013**, *173*, 74–84. [[CrossRef](#)]
34. Ghazaryan, G.; Dubovyk, O.; Graw, V.; Kussul, N.; Schellberg, J. Local-Scale Agricultural Drought Monitoring with Satellite-Based Multi-Sensor Time-Series. *GIScience Remote Sens.* **2020**, *57*, 704–718. [[CrossRef](#)]
35. Das, A.C.; Noguchi, R.; Ahamed, T. An Assessment of Drought Stress in Tea Estates Using Optical and Thermal Remote Sensing. *Remote Sens.* **2021**, *13*, 2730. [[CrossRef](#)]
36. AlJawa, S.B.; Al-Ansari, N. Open Access Online Journal of the International Association for Environmental Hydrology assessment of groundwater quality using. *Groundw. Qual. Using* **2017**, *26*, 1–14.
37. Al-quraishi, A.M.F.; Negm, A.M. *Environmental Remote Sensing and GIS in Iraq*; Springer: Berlin/Heidelberg, Germany, 2019; ISBN 9783030213435.
38. Phiri, D.; Simwanda, M.; Salekin, S.; Nyirenda, V.R.; Murayama, Y.; Ranagalage, M. Sentinel-2 Data for Land Cover/Use Mapping: A Review. *Remote Sens.* **2020**, *12*, 2291. [[CrossRef](#)]
39. Mahdianpari, M.; Salehi, B.; Mohammadimanesh, F.; Homayouni, S.; Gill, E. The First Wetland Inventory Map of Newfoundland at a Spatial Resolution of 10 m Using Sentinel-1 and Sentinel-2 Data on the Google Earth Engine Cloud Computing Platform. *Remote Sens.* **2019**, *11*, 43. [[CrossRef](#)]
40. Yengoh, G.T.; Dent, D.; Olsson, L.; Tengberg, A.E.; Tucker, C.J. *Use of the Normalized Difference Vegetation Index (NDVI) to Assess Land Degradation at Multiple Scales: A Review of the Current Status, Future Trends, and Practical Considerations*; Springer: Berlin/Heidelberg, Germany, 2014; ISBN 978-3-319-24110-4.
41. Hunt, E.R.; Rock, B.N. Detection of Changes in Leaf Water Content Using Near- and Middle-Infrared Reflectances. *Remote Sens. Environ.* **1989**, *30*, 43–54. [[CrossRef](#)]
42. Anderson, R.G.; French, A.N. Crop Evapotranspiration. *Agronomy* **2019**, *9*, 614. [[CrossRef](#)]
43. Kharrou, M.H.; Simonneaux, V.; Er-raki, S.; Page, M.L.; Khabba, S.; Chehbouni, A. Assessing Irrigation Water Use with Remote Sensing-based Soil Water Balance at an Irrigation Scheme Level in a Semi-arid Region of Morocco. *Remote Sens.* **2021**, *13*, 1133. [[CrossRef](#)]
44. Anyamba, A.; Tucker, C.J. Historical Perspectives on AVHRR NDVI and Vegetation Drought Monitoring. *Remote Sens. Drought Innov. Monit. Approaches* **2012**, *23*, 20. [[CrossRef](#)]
45. Mukherjee, A.; Wang, S.Y.S.; Promchote, P. Examination of the Climate Factors That Reduced Wheat Yield in Northwest India during the 2000s. *Water* **2019**, *11*, 343. [[CrossRef](#)]
46. Aquino, D.d.N.; Neto, O.C.d.R.; Moreira, M.A.; Teixeira, A.d.S.; de Andrade, E.M. Use of Remote Sensing to Identify Areas at Risk of Degradation in the Semi-Arid Region. *Rev. Cienc. Agron.* **2018**, *49*, 420–429. [[CrossRef](#)]
47. Pedro-Monzonis, M.; Solera, A.; Ferrer, J.; Estrela, T.; Paredes-Arquiola, J. A Review of Water Scarcity and Drought Indexes in Water Resources Planning and Management. *J. Hydrol.* **2015**, *527*, 482–493. [[CrossRef](#)]

48. Maimaitijiang, M.; Sagan, V.; Sidike, P.; Hartling, S.; Esposito, F.; Fritschi, F.B. Soybean Yield Prediction from UAV Using Multimodal Data Fusion and Deep Learning. *Remote Sens. Environ.* **2020**, *237*, 111599. [[CrossRef](#)]
49. Taghvaeian, S.; Neale, C.M.U.; Osterberg, J.C.; Sritharan, S.I.; Watts, D.R. Remote Sensing and GIS Techniques for Assessing Irrigation Performance: Case Study in Southern California. *J. Irrig. Drain. Eng.* **2018**, *144*, 05018002. [[CrossRef](#)]
50. Elmetwalli, A.H.; Mazrou, Y.S.A.; Tyler, A.N.; Hunter, P.D.; Elsherbiny, O.; Yaseen, Z.M.; Elsayed, S. Assessing the Efficiency of Remote Sensing and Machine Learning Algorithms to Quantify Wheat Characteristics in the Nile Delta Region of Egypt. *Agriculture* **2022**, *12*, 332. [[CrossRef](#)]
51. Ali, M.H. *Practices of Irrigation & On-Farm Water Management: Volume 2*; Springer Science & Business Media: Berlin/Heidelberg, Germany, 2011; ISBN 9781441976369.
52. Abuzar, M.; Whitfield, D.; McAllister, A.; Sheffield, K. Application of ET-NDVI-Relationship Approach and Soil-Water-Balance Modelling for the Monitoring of Irrigation Performance of Treed Horticulture Crops in a Key Fruit-Growing District of Australia. *Int. J. Remote Sens.* **2019**, *40*, 4724–4742. [[CrossRef](#)]
53. Mahmoud, S.H.; Gan, T.Y. Irrigation Water Management in Arid Regions of Middle East: Assessing Spatio-Temporal Variation of Actual Evapotranspiration through Remote Sensing Techniques and Meteorological Data. *Agric. Water Manag.* **2019**, *212*, 35–47. [[CrossRef](#)]
54. Gadédjisso-Tossou, A.; Avellán, T.; Schütze, N. Potential of Deficit and Supplemental Irrigation under Climate Variability in Northern Togo, West Africa. *Water* **2018**, *10*, 1803. [[CrossRef](#)]
55. Ma, C.; Johansen, K.; McCabe, M.F. Monitoring Irrigation Events and Crop Dynamics Using Sentinel-1 and Sentinel-2 Time Series. *Remote Sens.* **2022**, *14*, 1205. [[CrossRef](#)]
56. Karamage, F.; Zhang, C.; Fang, X.; Liu, T.; Ndayisaba, F.; Nahayo, L.; Kayiranga, A.; Nsengiyumva, J.B. Modeling Rainfall-Runoffresponse to Land Use and Land Cover Change in Rwanda (1990–2016). *Water* **2017**, *9*, 147. [[CrossRef](#)]
57. Armitage, F.B. *Irrigated Forestry in Arid and Semi-Arid Lands: A Synthesis*; IDRC: Ottawa, ON, USA, 1986; Volume 61, ISBN 088936432X.
58. Nouri, H.; Beecham, S.; Anderson, S.; Nagler, P. High Spatial Resolution WorldView-2 Imagery for Mapping NDVI and Its Relationship to Temporal Urban Landscape Evapotranspiration Factors. *Remote Sens.* **2013**, *6*, 580–602. [[CrossRef](#)]
59. Moran, M.S.; Clarke, T.R.; Inoue, Y.; Vidal, A. Estimating Crop Water Deficit Using the Relation between Surface-Air Temperature and Spectral Vegetation Index. *Remote Sens. Environ.* **1994**, *49*, 246–263. [[CrossRef](#)]
60. Bryla, D.R. Crop evapotranspiration and irrigation scheduling in blueberry. In *Evapotranspiration—From Measurements to Agricultural and Environmental Applications*; Intech: Rijeka, Croatia, 2011; pp. 167–186.

**Disclaimer/Publisher’s Note:** The statements, opinions and data contained in all publications are solely those of the individual author(s) and contributor(s) and not of MDPI and/or the editor(s). MDPI and/or the editor(s) disclaim responsibility for any injury to people or property resulting from any ideas, methods, instructions or products referred to in the content.